Optimal Sensor Placement for Agent Localization

DAMIEN B. JOURDAN and NICHOLAS ROY
Massachusetts Institute of Technology

In this paper we consider deploying a sensor network to help an agent navigate in an area. In particular the agent uses range measurements to the sensors to localize itself. We wish to place the sensors in order to provide optimal localization accuracy to the agent.

We begin by considering the problem of placing sensors in order to optimally localize the agent at a *single* location. The Position Error Bound (PEB), a lower bound on the localization accuracy, is used to measure the quality of sensor configurations. We then present RELOCATE, an iterative algorithm that places the sensors so as to minimize the PEB at that point.

When the range measurements are unbiased and have constant variances, we introduce a coordinate transform that allows us to obtain a closed-form solution to minimizing the PEB along one coordinate. We also prove that RELOCATE converges to the global minimum, and we compute the approximate expected rate of convergence of the algorithm. We then apply RELOCATE to the more complex case where the variance of the range measurements depends on the sensors location and where those measurements can be biased.

We finally apply RELOCATE to the case where the PEB must be minimized not at a single point, but at *multiple* locations, so that good localization accuracy is ensured as the agent moves through the area. We show that, compared to Simulated Annealing, the algorithm yields better results faster on these more realistic scenarios. We also show that by optimally placing the sensors, significant savings in terms of number of sensors used can be achieved. Finally we illustrate that the PEB is not only a convenient theoretical lower bound, but that it can actually be closely approximated by a maximum likelihood estimator.

Categories and Subject Descriptors: G.1.6 [**Numerical Analysis**]: Optimization; G.4 [**Mathematical Software**]: Algorithm analysis, Efficiency ; I.1.2 [**Algebraic Manipulation**]: Algorithms; I.6.3 [**Simulation and Modeling**]: Applications; J.2 [**Physical Sciences and Engineering**]: Engineering

General Terms: Algorithms

Additional Key Words and Phrases: Localization, sensor placement, target location, tracking, Ultra-Wideband (UWB).

Author's address: D. B. Jourdan, Laboratory for Information and Decision Systems (LIDS), Massachusetts Institute of Technology (MIT), 77 Massachusetts Avenue, Room 32-D740, Cambridge, MA 02139, USA (e-mail: jourdan@mit.edu).

N. Roy, Computer Science and Artificial Intelligence Laboratory (CSAIL), Massachusetts Institute of Technology, Room 32-315, 77 Massachusetts Avenue, Cambridge, MA 02139, USA (e-mail: nickroy@mit.edu).

This research was supported by the Charles Stark Draper Laboratory Robust Distributed Sensor Networks Program.

1. INTRODUCTION

1.1 Motivation

There has been considerable work devoted to the target localization problem, where the target position is to be determined from a set of possibly noisy measurements [Bar-Shalom et al. 2001; Fox et al. 1999; Minvielle 2005; Jourdan et al. 2005]. We focus in this paper on range-only localization, where the measurements used to locate the target are range estimates between the target and a set of stationary sensors. These range measurements can be obtained via acoustic or electro-magnetic media (e.g. sonar [Leonard and Durrant-Whyte 1992; Tardós et al. 2002], or radar [Skolnik 1980; Bar-Shalom et al. 2001]). Because the so-called "target" is not necessarily hostile, we refer to it instead as an "agent." We consider a mission scenario where accurate localization must be enabled in a specific area. For example we may want to provide a robot with its position at all times as it moves inside a building. Sensors would then be deployed to designated locations around the building (e.g. from the outside using human personnel or airdrops via an aircraft), in order to provide the necessary indoor coverage.

The effect of the sensors' geometry on the quality of the position estimate is well-known. Clustering all sensors together will yield poor position observability. Likewise, the range measurements typically degrade with distance, so that sensors near the agent will provide more reliable information than those further away. The Geometric Dilution of Precision (GDOP) has been used and studied extensively, notably by the GPS community to assess the quality of different satellite configurations [Spilker 1978; Yarlagadda et al. 2000; Chaffee and Abel 1994]. The Information Inequality [Bickel and Doksum 2001] is also a popular means of deriving measures of localization accuracy that combines both the sensors' geometry and the statistical properties of the measurements. The Position Error Bound (PEB) was derived in [Jourdan et al. 2006] using the Information Inequality for an indoor localization system using Ultra-Wideband (UWB) ranging sensors. Because of its generality, the PEB will be used in this paper to measure the quality of sensors configurations.

Although the effect of geometry is well-known, there is comparatively little work on the optimization of sensor placement. Given a region of interest, the challenge is to find the layout of sensors that will provide maximum localization quality. In this paper we develop RELOCATE, a coordinate-descent algorithm, and demonstrate theoretically and through numerical simulations that this approach is well-suited for the optimal sensor placement problem.

In Section 2 we first model the range measurements and define the PEB. Then RELOCATE, the placement algorithm, is presented. In Section 3 we apply RELOCATE to the single agent location problem where the range measurements are unbiased and have constant (but possibly different) variances. We introduce the coordinate transform that allows us to prove key results, in particular that RELOCATE converges to the global minimum efficiently. An algorithm solving this placement problem has been proposed in [Zhang 1995], but that method cannot be easily extended beyond that simple case. Our goal in this section will be to gain confidence in our algorithm before generalizing it to more complex cases. The coordinate transform is also critical for deriving an expected rate of convergence, so that our algorithm is shown to converge in practice with great precision in only a few steps, even for a large number of sensors.

In Section 4 we adapt our algorithm to deal with the more realistic case where the range measurements can be biased and their variance depends on the sensor location, something

not present to our knowledge in the literature. For example the measurement variance may increase with the distance to the agent, or when obstacles obstruct the line-of-sight between agent and sensors. In Section 5 we then consider the case where instead of minimizing the PEB at a single location (which does not have many realistic applications), the *average* PEB over *multiple* agent locations is to be minimized. For example the agent may be moving through the area and good localization must be provided along its trajectory. In such situations the quality of the range measurements may also vary with sensor position, so this case is the most general. We show that our algorithm performs well on this realistic scenario by comparing its performance to Simulated Annealing (SA) [Kirkpatrick et al. 1983]. SA is a natural choice for such combinatorial optimization problems, and it has been used on the sensor placement problem before [Chiu and Lin 2004]. We also show that by carefully planning the sensor placement, fewer sensors are required to achieve the same accuracy than one-size-fits-all approaches such as distributing the sensors evenly on the area boundary. Finally we show that the PEB is not only a convenient theoretical lower bound, but that it can actually be closely approximated by a maximum likelihood estimator.

In this paper we restrict ourselves to static sensors operating in 2D. We initially restrict the sensors to lie on the boundary of a compact set, with the agent in its interior as in [Martínez and Bullo 2004]. These assumptions are in accordance with our mission scenario where localization must be provided inside an area, while the sensors are deployed from outside that area. However we will also apply our algorithm later on to the case where the agent moves between different buildings with sensors placed on the buildings' walls.

Related Work

McKay and Pachter [1997] and Hegazy and Vachtsevanos [2003] minimize the condition number of the visibility matrix in order to minimize the impact of range measurement errors on the position estimate. In both [McKay and Pachter 1997] and [Hegazy and Vachtsevanos 2003], three dimensions are considered, although in [McKay and Pachter 1997] the sensors are constrained to lie on the ground. A Sequential Quadratic Programming method is used to solve the problem in [McKay and Pachter 1997], while in [Hegazy and Vachtsevanos 2003] an analytical solution is derived for 4 sensors. Sinha et al. [2004] maximizes the Fisher information gathered by a group of sensor UAVs, which blends sensor geometry, survivability, and distance to the target. A Genetic Algorithm coupled with a gradient descent algorithm is used to search for the global minimum.

Abel [1990], Martínez and Bullo [2004], and Zhang [1995] optimize the sensor placement by minimizing a cost related to the Cramér-Rao bound (CRB), obtained from the Information Inequality. The acoustic sensors are constrained to lie on a line segment in [Abel 1990], which allows for a simple analytic solution. Martínez and Bullo [2004] derive an analytic form for the CRB in 2D and 3D for the case where all the sensors have similar measurement variance. The classic result is found, namely that the configuration with minimum CRB is that with all sensors evenly spread around the agent [Levanon 2000]. The authors then use this result to dynamically control the sensors in order to track a moving agent. Finally Zhang [1995] considers the optimal placement of sensors in 2D, where the sensors have different measurement variances. He minimizes the determinant of the joint covariance matrix, which turns out to be equivalent to minimizing the CRB. Zhang then obtains the minimum value of the CRB for this case and proposes an algorithm that converges to the optimal sensor placement in *n-3* steps (where *n* is the number of sensors). Zhang's algorithm, however, does not generalize beyond the case of constant variances,

which limits its applicability to more realistic scenarios.

Most of these papers are restricted to optimizing the sensor placement for the localization of a single agent location. A possible exception is [Martínez and Bullo 2004] since the agent can move, but in this case the sensors are mobile and can adaptively rearrange their configuration. Sheng and Hu [2003] consider the placement of static sensors for the localization of an agent along its path, but the approach is more statistical in nature and assumes that many sensors can be deployed.

2. PRELIMINARIES AND NOTATIONS

2.1 Modeling of the Range Measurements

We consider a system of n range sensors. In the literature these range measurements are typically assumed to be unbiased, normally distributed independent variables with constant variances [Abel 1990; Martínez and Bullo 2004; Zhang 1995]. In this paper we consider a more general model for the measurements that does not restrict them to be normally distributed or unbiased. In particular, we base our modeling on results obtained with Ultra-Wideband (UWB) range sensors [Jourdan et al. 2005]. UWB technology potentially provides high ranging accuracy in cluttered environments [Low et al. 2005; Falsi et al. 2006; Gezici et al. 2005; Lee and Scholtz 2002] (such as indoor or urban environments), owing to its inherent fine delay resolution and ability to penetrate obstacles [Win and Scholtz 1998b; 1998a; Cassioli et al. 2002; Win and Scholtz 2002]. It is therefore an excellent candidate technology for range measurements, outdoors and indoors. As described more in depth in [Jourdan et al. 2006], the range measurement $\tilde{r}_k$ of the k^{th} sensor can be expressed as

$$\tilde{r}_k = d_k + b_k + \epsilon_k, \tag{1}$$

where d_k is the true distance between the sensor and the agent, b_k is a positive bias, and ϵ_k is a random Gaussian noise. Although the biases b_k can be distributed according to any type of staircase diagram [Jourdan et al. 2006], we assume here that the biases are uniformly distributed between 0 and β_k. This is without loss of generality, as the algorithm presented in this paper can easily accommodate more general distributions. The Gaussian noises ϵ_k are independent of b_k, with zero-mean and variance σ_k^2. We model their dependence on the distance d_k as

$$\sigma_k^2(d_k) = \sigma_{0k}^2 d_k^{\alpha}, \tag{2}$$

where $\alpha \geq 0$ is the path-loss exponent and σ_0^2 is the variance at one meter [Gezici et al. 2005; Cassioli et al. 2002].

Let r_k be the *debiased* range measurement (i.e. $r_k = \tilde{r}_k - E\{\tilde{r}_k\}$). The probability density function (pdf) of r_k given the true distance d_k is then [Jourdan et al. 2006]

$$f_k(r_k|d_k) = \frac{1}{\beta_k}\left[Q\left(\frac{r_k - d_k - \beta_k/2}{\sigma\left(d_k\right)}\right) - Q\left(\frac{r_k - d_k + \beta_k/2}{\sigma\left(d_k\right)}\right)\right], \tag{3}$$

where $Q(x) = \frac{1}{\sqrt{2\pi}}\int_x^{+\infty} e^{-t^2/2}dt$ is the Gaussian Q function. This expression is general in that it allows the range measurement to be biased (as is often the case due to non-line-of-sight (NLOS) propagation), and the range measurement variance to vary with the distance. The pdf is plotted on Figure 1 for $d_k = 15m$ and $\beta_k = 2m$. The expression in (3) can be

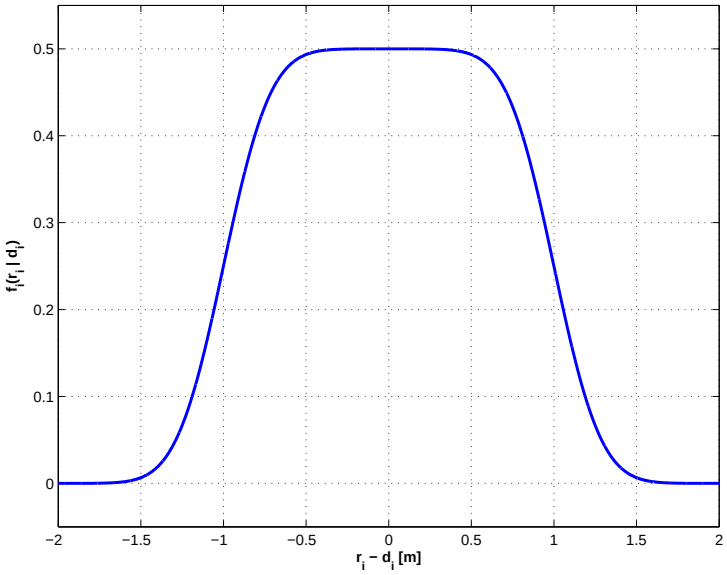

Fig. 1. Probability density function of the debiased error in range measurements $r_i - d_i$ given the true distance $d_i = 15m$, $\alpha = 2$, $\sigma_0 = 1mm$, and $\beta_i = 2m$. With these parameters the error is approximates a uniform distribution of size 2m

easily specialized to the case when there is no bias in the measurements ($\beta_k = 0$), so that

$$f_k(r_k|d_k) = \frac{1}{\sqrt{2\pi}\sigma_k(d_k)} e^{-\frac{(r_k-d_k)^2}{2\sigma_k^2(d_k)}}. \tag{4}$$

If in addition the measurement variance does not depend on the distance as is commonly assumed, then

$$f_k(r_k|d_k) = \frac{1}{\sqrt{2\pi}\sigma_{0k}} e^{-\frac{(r_k-d_k)^2}{2\sigma_{0k}^2}}, \tag{5}$$

and we obtain the model typically assumed in the literature, i.e., where the measurements are unbiased and normally distributed with constant variance.

2.2 The Design Variables $\boldsymbol{\theta}$

We will constrain the sensors to lie on the boundary of a set (representing for example the exterior walls of a building). Initially we assume this set to be convex, with the agent in its interior. In this case the position of the sensor is completely determined by θ_k, the angle the agent makes with the k^{th} sensor, as shown on Figure 2. The design variables to be optimized are the sensor locations, denoted by the vector $\boldsymbol{\theta} = (\theta_1, \ldots, \theta_n)$. The convexity assumption of the set is for convenience, and will be relaxed later on in this paper, when for example sensors can be placed on walls belonging to different buildings. In that case the angles θ_k are not sufficient to unambiguously characterize the sensors positions and another parametrization should then be used.

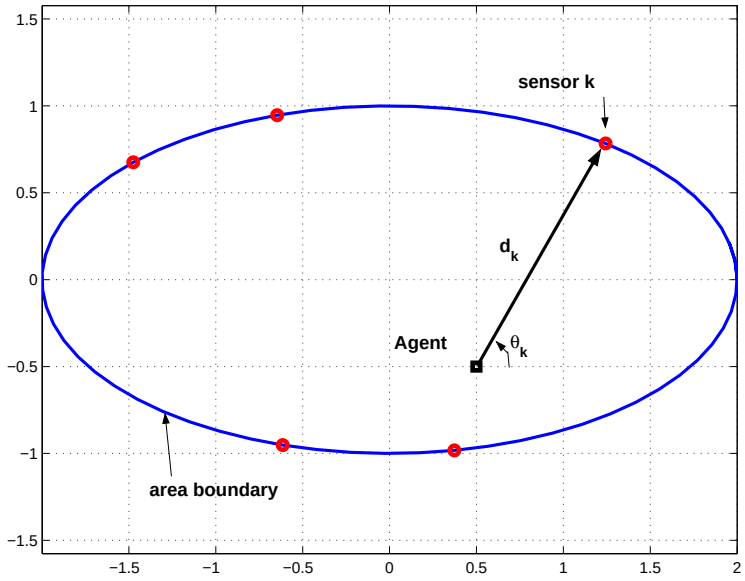

Fig. 2. The agent (square) is inside a convex area, and the sensors (circles) are placed on its boundary. Because we assume the boundary is convex, the sensor location can be parametrized by the angle θ_k, with the distance between the agent and sensor k depending only on θ_k.

2.3 The Position Error Bound (PEB)

The PEB is a lower bound on the localization accuracy of any unbiased position estimator, so it is a natural choice to measure the quality of sensor configurations. In particular we have

$$\sqrt{\mathbb{E}_{\mathbf{r}}\left\{(x-\hat{x})^2+(y-\hat{y})^2\right\}} \geq \mathsf{PEB} \tag{6}$$

for any estimator $(\hat{x},\hat{y})$ of the true agent's position (x,y), where $\mathbb{E}_{\mathbf{r}}$ denotes the expectation taken over the range measurements $\mathbf{r}$[1]. Although the range measurement model described above is quite general, it is possible to obtain a closed-form expression for the PEB through calculation of the classic Fisher Information matrix [Bickel and Doksum 2001]. We refer the reader to [Jourdan et al. 2006] for a detailed derivation. We obtain

$$\mathsf{PEB}\left(\boldsymbol{\theta}\right) = \sqrt{\frac{\sum_{k=1}^{n}[A_k(\theta_k)]}{\sum_{k=1}^{n}[A_k(\theta_k)\cos^2\theta_k]\sum_{k=1}^{n}[A_k(\theta_k)\sin^2\theta_k]-\left(\sum_{k=1}^{n}[A_k(\theta_k)\cos\theta_k\sin\theta_k]\right)^2}}, \tag{7}$$

where

$$A_k(\theta_k) = \frac{1}{\beta_k\sigma_k(d_k)\pi\sqrt{2}}\int_{-\infty}^{\infty} h(y,\beta_k,d_k)dy, \tag{8}$$

[1]If $\hat{R}=\sqrt{(x-\hat{x})^2+(y-\hat{y})^2}$ is the distance error between the true position and an estimated position $(\hat{x},\hat{y})$, then the PEB is a lower bound on the mean-square error (MSE) of this distance.

with

$$h(y,\beta,d)=\frac{\left[\left(e^{-y^2}-e^{-\left(y+\frac{\beta}{\sigma(d)\sqrt{2}}\right)^2}\right)\left(1+\frac{\alpha\sigma(d)}{d\sqrt{2}}y\right)-\frac{\alpha\beta}{2d}e^{-\left(y+\frac{\beta}{\sigma(d)\sqrt{2}}\right)^2}\right]^2}{Q(\sqrt{2}y)-Q\left(\sqrt{2}y+\frac{\beta}{\sigma(d)}\right)}. \quad (9)$$

The coefficient $A_k(\theta_k)$ is called the *importance weight* of the k^{th} sensor. Note that when there is no bias, we have

$$A_k(\theta_k)=\frac{1}{\sigma_{0k}^2 d_k^{\alpha}(\theta_k)}+\frac{\alpha^2}{2d_k^2(\theta_k)}. \quad (10)$$

If in addition $\alpha=0$ and all the standard deviations are equal, the PEB is simply equal to the GDOP multiplied by the standard deviation of the range measurements. In that case all the range measurements are equally weighted (by $1/\sigma_0^2$), and minimizing the PEB is equivalent to minimizing the GDOP. In fact it is well-known that the minimum GDOP in this case is obtained when the sensors are placed at the vertices of a regular polygon centered around the agent [Levanon 2000].

When α or β are non-zero, however, equation (8) implies that the range measurements from different sensors will not be equally weighted in the PEB. Some sensors will have large importance weights due to favorable propagation characteristics between the agent and the sensor, or because they are close to one another. Others will receive a low weight, for example if the distance between agent and sensor is large, or if the propagation environment is harsh (e.g. much clutter). Minimizing the PEB therefore implies striking the optimal balance between spatial diversity (captured by the sine and cosine in (7)) and range measurement quality (captured by the importance weights). This non-trivial task requires using an optimization algorithm[2].

2.4 Generic Algorithm Description

We now present the RELOCATE algorithm in its generic form. We omit for the time being some additional conditions required to guarantee convergence to the *optimal* solution. This algorithm is a coordinate descent algorithm, i.e., it minimizes the PEB one coordinate at a time, until convergence. It operates as follows:

RELOCATE

—Randomly initialize $\boldsymbol{\theta}^1=\{\theta_1^1,...\theta_n^1\}$, $p=1$;

—Until convergence, do:

(1) Select sensor i_p for relocation;
(2) Find the angle $\theta_{i_p}^*$ that minimizes the PEB along θ_{i_p};
(3) Set $\theta_{i_p}^{p+1}=\theta_{i_p}^*$ and $\theta_k^{p+1}=\theta_k^p$ for all $k\neq i_p$, so that $\boldsymbol{\theta}^{p+1}=\left(\theta_1^p,\ldots,\theta_{i_p}^*,\ldots,\theta_n^p\right)$;
(4) $p\leftarrow p+1$.

Coordinate descent algorithms are efficient as long as the minimization in step (2) is fast [Bertsekas 2003], i.e., as long as finding $\theta_{i_p}^*$ such that $\frac{\partial \mathsf{PEB}}{\partial\theta_{i_p}}(\theta_{i_p}^*)=0$ and $\frac{\partial^2 \mathsf{PEB}}{\partial\theta_{i_p}^2}(\theta_{i_p}^*)\geq 0$ is easy. In the following section we show that step (2) can in fact be solved in *closed-form*

[2] the PEB is a *lower bound* on the localization accuracy, and a discussion on its achievability is provided in section 5.4

when the importance weights are constant. This result, along with others on convergence and rate of convergence, will be made possible through the coordinate transform introduced next.

3. SINGLE AGENT LOCATION AND SENSORS WITH CONSTANT IMPORTANCE WEIGHTS

Let us consider the case where the importance weights $A_k(\theta_k)$ do not depend on θ_k, that is, the weights are independent of where the sensors are located. This can be the case for example if we assume that the variance of the range measurements is constant ($\alpha = 0$) and there are no biases ($\beta = 0$), which is the typical assumption in the literature. From (7) we see that in this case the PEB is the same for angles modulo π, so we will only consider values of θ_k between 0 and π. We also assume without loss of generality that $A_n \geq ... \geq A_1$.

3.1 Coordinate Transform

Instead of working directly with the angles θ_i, we introduce a set of complex numbers (or vectors) $\mathbf{r}(\boldsymbol{\theta})$ and $\mathbf{z_i}(\boldsymbol{\theta})$ for $i = 1, \ldots, n$. This representation will be critical in allowing us to solve step (2) of RELOCATE in closed-form, to prove the optimal convergence of the algorithm, and to approximate its expected rate of convergence.

Definition 3.1 *Coordinate transform*.

$$\mathbf{z_i}(\boldsymbol{\theta}) \;=\; e^{-2j\theta_i} \sum_{k \neq i} A_k e^{2j\theta_k}, \quad \forall\, i = 1 \ldots n, \tag{11}$$

$$\mathbf{r}(\boldsymbol{\theta}) \;=\; \sum_{k=1}^{n} A_k e^{2j\theta_k}, \tag{12}$$

$$r(\boldsymbol{\theta}) \;=\; |\mathbf{r}(\boldsymbol{\theta})|, \tag{13}$$

where j denotes the complex number such that $j^2 = -1$.

In particular we will show that if the PEB is minimum at $\tilde{\boldsymbol{\theta}}$, we must have $\Re\left\{\mathbf{z_i}(\tilde{\boldsymbol{\theta}})\right\} \leq 0$ and $\Im\left\{\mathbf{z_i}(\tilde{\boldsymbol{\theta}})\right\} = 0$ for all i, in other words all the $\mathbf{z_i}(\tilde{\boldsymbol{\theta}})$ must lie on the negative real axis[3].

3.2 Graphical interpretaiton of the coordinate transform

Following the definitions of the coordinate transorm, let us derive results that will be helpful for visualizing the complex vectors and using them in the subsequent proofs.

LEMMA 3.2 FUNDAMENTAL RELATIONSHIPS. *The following relationships hold:*

$$\mathbf{z_i}(\boldsymbol{\theta}) + A_i \;=\; e^{-2j\theta_i}\mathbf{r}(\boldsymbol{\theta}), \quad \forall\, i = 1, \ldots, n \tag{14}$$

$$r(\boldsymbol{\theta}) \;=\; |\mathbf{z_i}(\boldsymbol{\theta}) + A_i|, \quad \forall\, i = 1, \ldots, n \tag{15}$$

PROOF. These results follow directly from the definitions. □

COROLLARY 3.3. *For $k = 1, \ldots, n$, $\mathbf{z_k}(\boldsymbol{\theta})$ is the vector starting at $(0, 0)$ and ending on the circle of radius $r(\boldsymbol{\theta})$, centered at $(-A_k, 0)$.*

[3]where $\Re\{a\}$ and $\Im\{a\}$ respectively are the real and imaginary parts of a, a complex number.

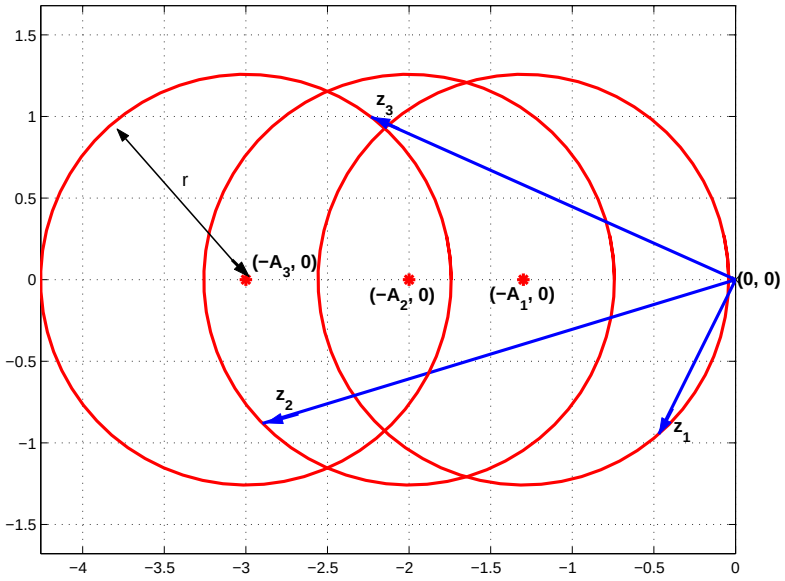

Fig. 3. Plot of the $\mathbf{z_k}(\boldsymbol{\theta})$ for 3 sensors, with $A_1 = 1.3$, $A_2 = 2$ and $A_3 = 3$. Note that the 3 vectors lie on the circles of equal radius (equal to $r(\boldsymbol{\theta}) = |A_k + \mathbf{z_k}(\boldsymbol{\theta})|$) centered on $(-A_k, 0)$, for $k = 1 \ldots 3$.

PROOF. This follows from (14), which states that $\mathbf{z_k}(\boldsymbol{\theta})$ is obtained by rotating vector $\mathbf{r}(\boldsymbol{\theta})$ by $-2\theta_k$, and adding vector $(-A_k, 0)$ to it (the latter is equivalent to a translation along the negative real axis). □

COROLLARY 3.4. *If θ_i is varied while all other θ_k remain fixed, $\mathbf{z_i}(\boldsymbol{\theta})$ rotates about $(0, 0)$ by an angle $-2\theta_i$, but* its magnitude does not change. *However all the other $\mathbf{z_k}(\boldsymbol{\theta})$ rotate* and *change magnitude as θ_i varies.*

PROOF. Equation (11) states that $\mathbf{z_i}(\boldsymbol{\theta})$ depends on θ_i only through $e^{-2j\theta_i}$, which appears as a factored term, so that the norm of θ_i does not depend on θ_i. For all the other vectors however, the dependence on θ_i is through $A_i e^{-2j\theta_i}$, which is inside the sum and cannot be factored out. □

COROLLARY 3.5. *Let $\boldsymbol{\theta} = (\theta_1, \ldots, \theta_i, \ldots, \theta_n)$. If θ_i is changed to $\tilde{\theta}_i$ such that $\mathbf{z_i}(\tilde{\theta})$ lies on the real axis (with $\tilde{\boldsymbol{\theta}} = (\theta_1, \ldots, \tilde{\theta}_i, \ldots, \theta_n)$), then the resulting $r(\tilde{\boldsymbol{\theta}})$ is equal to $|A_i - |\mathbf{z_i}(\boldsymbol{\theta})||$, i.e. it does not explicitly depend on the actual value of the new $\tilde{\theta}_i$.*

PROOF. According to Corollary 3.4, when θ_i varies to $\tilde{\theta}_i$ the magnitude of $\mathbf{z_i}(\tilde{\boldsymbol{\theta}})$ does not change, so that $|\mathbf{z_i}(\tilde{\boldsymbol{\theta}})| = |\mathbf{z_i}(\boldsymbol{\theta})|$. Also, according to Corollary 3.3 the tip of $\mathbf{z_i}(\tilde{\boldsymbol{\theta}})$ is on the circle of radius $r(\tilde{\boldsymbol{\theta}})$ centered at $(-A_i, 0)$. But since both $(-A_i, 0)$ and $\mathbf{z_i}(\tilde{\boldsymbol{\theta}})$ are on the real axis, we have $|\mathbf{z_i}(\tilde{\boldsymbol{\theta}}) + A_i| = |A_i - |\mathbf{z_i}(\tilde{\boldsymbol{\theta}})||$, which by (15) is equal to $r(\tilde{\boldsymbol{\theta}})$. □

These corollaries help to to visualize the vectors $\mathbf{z_k}(\boldsymbol{\theta})$ and $\mathbf{r}(\boldsymbol{\theta})$ in the plane. This is illustrated in Figure 3 for 3 sensors. The sensors are placed at θ_1, θ_2 and θ_3, and the A_k are assumed constant with $A_3 = 3$, $A_2 = 2$, and $A_1 = 1.3$. As indicated in Corollary 3.3, the 3 corresponding vectors $\mathbf{z_1}(\boldsymbol{\theta})$, $\mathbf{z_2}(\boldsymbol{\theta})$, and $\mathbf{z_3}(\boldsymbol{\theta})$ all lie on circles of equal radius $r(\boldsymbol{\theta})$, respectively centered at $(-A_1, 0)$, $(-A_2, 0)$, and $(-A_3, 0)$.

If θ_3 varies while θ_1 and θ_2 remain fixed, $\mathbf{z_3}(\boldsymbol{\theta})$ will rotate about $(0,0)$ with its magnitude unchanged (Corollary 3.4). Note that since the tip of this vector must always lie on the circle of radius $r(\boldsymbol{\theta})$ centered at $(-A_3, 0)$, this radius will change as $\mathbf{z_3}(\boldsymbol{\theta})$ rotates. Note in particular that $r(\boldsymbol{\theta})$ *will be minimum when* $\mathbf{z_3}(\boldsymbol{\theta})$ *lies on the negative real axis*. In that case the radius is then equal to $|A_3 - |\mathbf{z_3}(\boldsymbol{\theta})||$ (Corollary 3.5). This is an important observation that will be key to proving the correctness of RELOCATE.

Note that Corollary 3.9 is in accordance with our observation about Fig. 3: when rotating $\mathbf{z_i}$, the error radius is minimized when $\mathbf{z_i}$ lies on the negative real axis. This is just what θ_i^* does.

3.3 General Results on the PEB

The assumption of constant weights leads to two key results about the PEB. The first result, given in the following lemma, relates $r(\boldsymbol{\theta})$ to $\mathsf{PEB}\,(\boldsymbol{\theta})$.

LEMMA 3.6. *When the importance weights are constant, minimizing* $\mathsf{PEB}\,(\boldsymbol{\theta})$ *is equivalent to minimizing* $r(\boldsymbol{\theta})$*, and* $\mathsf{PEB}\,(\boldsymbol{\theta})$ *can be re-written as*

$$\mathsf{PEB}\,(\boldsymbol{\theta}) \;=\; \sqrt{\frac{4\sum_{k=1}^{n} A_k}{(\sum_{k=1}^{n} A_k)^2 - r^2(\boldsymbol{\theta})}}. \tag{16}$$

PROOF. Let us write

$$\begin{aligned}
\sum_{k=1}^{n}[A_k \cos^2\theta_k]\sum_{k=1}^{n}[A_k \sin^2\theta_k] \;&=\; \frac{1}{4}\sum_{k=1}^{n}[A_k(1+\cos 2\theta_k)]\sum_{k=1}^{n}[A_k(1-\sin 2\theta_k)] \\
&=\; \frac{1}{4}\left[\left(\sum_{k=1}^{n} A_k\right)^2 - \left(\sum_{k=1}^{n} A_k\cos 2\theta_k\right)\left(\sum_{k=1}^{n} A_k \sin 2\theta_k\right)\right] \\
&=\; \frac{1}{4}\left[\left(\sum_{k=1}^{n} A_k\right)^2 - \left(\sum_{k=1}^{n} A_k\cos 2\theta_k\right)^2\right]
\end{aligned}$$

Likewise we write

$$\left(\sum_{k=1}^{n} A_k \cos\theta_k \sin\theta_k\right)^2 \;=\; \frac{1}{4}\left(\sum_{k=1}^{n} A_k \sin 2\theta_k\right)^2$$

The denominator of (7) can therefore be written as

$$\begin{aligned}
denominator \;&=\; \frac{1}{4}\left[\left(\sum_{k=1}^{n} A_k\right)^2 - \left[\left(\sum_{k=1}^{n} A_k\cos 2\theta_k\right)^2 + \left(\sum_{k=1}^{n} A_k \sin 2\theta_k\right)^2\right]\right] &(17)\\
&=\; \frac{1}{4}\left[\left(\sum_{k=1}^{n} A_k\right)^2 - \left[\left(\Re\{r(\boldsymbol{\theta})\}\right)^2 + \left(\Re\{r(\boldsymbol{\theta})\}\right)^2\right]\right] &(18)\\
&=\; \frac{1}{4}\left[\left(\sum_{k=1}^{n} A_k\right)^2 - r^2(\boldsymbol{\theta})\right] &(19)
\end{aligned}$$

□

$r(\boldsymbol{\theta})$ therefore provides a measure of the distance to optimality, and so it will be referred to as the *error radius*. The following lemma gives a lower bound on the error radius.

LEMMA 3.7. *For any $\boldsymbol{\theta}$ we have*

$$r(\boldsymbol{\theta}) \geq r^* = \max(0, A_n - \sum_{k=1}^{n-1} A_k). \tag{20}$$

PROOF. Let us write:

$$\mathbf{r}(\boldsymbol{\theta}) = A_n e^{2j\theta_n} + \sum_{k=1}^{n-1} A_k e^{2j\theta_k} \tag{21}$$

The triangle inequality on this sum of two vectors gives

$$|\mathbf{r}(\boldsymbol{\theta})| = r(\boldsymbol{\theta}) \;\geq\; \left| \left|A_n e^{2j\theta_n}\right| - \left|\sum_{k=1}^{n-1} A_k e^{2j\theta_k}\right| \right| \tag{22}$$

$$\geq \left| A_n - \left|\sum_{k=1}^{n-1} A_k e^{2j\theta_k}\right| \right| \tag{23}$$

$$\geq\; A_n - \left|\sum_{k=1}^{n-1} A_k e^{2j\theta_k}\right| \tag{24}$$

Another application of the triangle inequality gives

$$\sum_{k=1}^{n-1} A_k = \sum_{k=1}^{n-1} A_k \left|e^{2j\theta_k}\right| \geq \left|\sum_{k=1}^{n-1} A_k e^{2j\theta_k}\right| \tag{25}$$

Combining (24) and (25) yields the desired result

$$r(\boldsymbol{\theta}) \;\geq\; A_n - \sum_{k=1}^{n-1} A_k \tag{26}$$

□

Therefore, if there exists $\tilde{\boldsymbol{\theta}}$ such that $r(\tilde{\boldsymbol{\theta}}) = r^*$, $\tilde{\boldsymbol{\theta}}$ is a global minimum of the PEB. In particular, if $A_n > \sum_{k=1}^{n-1} A_k$, the global minimum is easily found by setting (for example) $\theta_n = 0$ and $\theta_k = \pi/2$ for $k = 1, \ldots, n-1$. We will show in Section 3.4 that there always exists $\tilde{\boldsymbol{\theta}}$ such that $r(\tilde{\boldsymbol{\theta}}) = r^*$, and that it can be found using the proposed algorithm.

Step (2) of RELOCATE involves a 1-dimensional minimization of the PEB along θ_{i_p} (or equivalently a minimization of the error radius along θ_{i_p}). A typical shape of the PEB as a function of θ_{i_p} is plotted on Figure 4. As indicated on the figure, the PEB is a smooth function of θ_{i_p} with a unique minimum in $[0, \pi)$. The second key result, stated in the following lemma, gives the closed-form expression of this unique minimum.

LEMMA 3.8 CLOSED-FORM SOLUTION TO STEP (2) OF RELOCATE. *The minimization*

$$\theta_i^* = \arg \min_{\theta_i \in [0,\pi)} \{r(\theta_1, \ldots, \theta_i, \ldots, \theta_n)\}$$

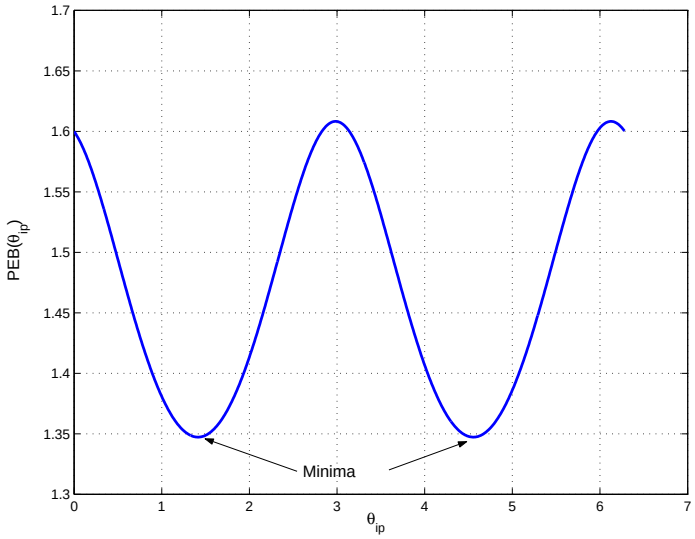

Fig. 4. Typical shape of $\mathsf{PEB}(\theta_{i_p})$ when the weights $A_k(\theta_k)$ are constant. Note that it has a unique minimum in $[0, \pi)$, showing that the one-dimensional minimization of the PEB along θ_i has a unique solution.

has a unique solution given by

$$\theta_i^* = \frac{1}{2}\arctan\left(\frac{\sum_{k\neq i} A_k \sin 2\theta_k}{\sum_{k\neq i} A_k \cos 2\theta_k}\right) + q\frac{\pi}{2}, \tag{27}$$

where $q \in \{0, 1\}$ *such that* $\Re\{\mathbf{z_i}(\theta_1, \ldots, \theta_i^*, \ldots, \theta_n)\} \leq 0$.

PROOF. We first write from (12)

$$r^2(\boldsymbol{\theta}) = |\sum_{k\neq i} A_k e^{2j\theta_k}|^2 + A_i^2 + 2A_i \sum_{k\neq i} A_k \cos(2\theta_k - 2\theta_i). \tag{28}$$

The minimum of $r(\theta_1, \ldots, \theta_i, \ldots, \theta_n)$ with respect to θ_i is the same as that of $r^2(\theta_1, \ldots, \theta_i, \ldots, \theta_n)$ and is found where the corresponding first partial derivative is 0 and the second derivative is non-negative. We first calculate

$$\begin{aligned}
\frac{\partial\left(r^2(\boldsymbol{\theta})\right)}{\partial\theta_i} &= 4A_i \sum_{k\neq i} A_k \sin(2\theta_k - 2\theta_i) && (29)\\
&= 4Ai\left[\left(\sum_{k\neq i} A_k \sin 2\theta_k\right)\cos 2\theta_i - \left(\sum_{k\neq i} A_k \cos 2\theta_k\right)\sin 2\theta_i\right] && (30)\\
&= 4A_i \Im\left\{\mathbf{z_i}(\boldsymbol{\theta})\right\}. && (31)
\end{aligned}$$

This is a sinusoidal function of θ_i, which is 0 twice in $[0, \pi)$. The two roots are given by

$$\theta_i^0 = \frac{1}{2}\arctan\left(\frac{\sum_{k\neq i} A_k \sin 2\theta_k}{\sum_{k\neq i} A_k \cos 2\theta_k}\right), \tag{32}$$

$$\theta_i^1 = \frac{1}{2}\arctan\left(\frac{\sum_{k\neq i} A_k \sin 2\theta_k}{\sum_{k\neq i} A_k \cos 2\theta_k}\right) + \frac{\pi}{2}. \tag{33}$$

By taking the derivative of (30) one more time with respect to θ_i we obtain

$$\frac{\partial^2\left(r^2(\boldsymbol{\theta})\right)}{\partial\theta_i^2} = -8A_i\left[\left(\sum_{k\neq i} A_k \sin 2\theta_k\right)\sin 2\theta_i + \left(\sum_{k\neq i} A_k \cos 2\theta_k\right)\cos 2\theta_i\right] \tag{34}$$

$$= -8Ai\Re\left\{\mathbf{z_i}(\boldsymbol{\theta})\right\}, \tag{35}$$

which is a sinusoidal function of θ_i that is non-positive at either θ_i^0 or θ_i^1 (but not both), depending on which one yields $\Re\left\{\mathbf{z_i}(\boldsymbol{\theta})\right\} \leq 0$. There is therefore a *unique* value of θ_i in $[0, \pi)$ for which (30) is 0 and (35) is non-negative, and $r(\boldsymbol{\theta})$ has a unique minimum along the i^{th} coordinate, obtained at θ_i^* given by (27). □

The following corollary follows from this proof.

COROLLARY 3.9. *If at iteration p RELOCATE selects sensor i_p for relocation, the corresponding $\mathbf{z_{i_p}}$ is rotated by $-2\theta_{i_p}^*$ so as to lie on the negative real axis, i.e.,*

$$\Re\left\{\mathbf{z_{i_p}}(\theta_1^p, \ldots, \theta_{i_p}^*, \ldots, \theta_n^p)\right\} \leq 0 \text{ and } \Im\left\{\mathbf{z_{i_p}}(\theta_1^p, \ldots, \theta_{i_p}^*, \ldots, \theta_n^p)\right\} = 0.$$

We also have the following result.

COROLLARY 3.10. *The stationary points of the PEB are such that all $\mathbf{z_i}$ lie on the real axis. Moreover candidates for minima are those stationary points for which all $\mathbf{z_i}$ lie on the* negative *real axis.*

PROOF. At a stationary point $\tilde{\boldsymbol{\theta}}$ of the PEB, the gradient of the PEB with respect to $\boldsymbol{\theta}$ is the zero vector. In other words, all the first partial derivatives $\frac{\partial \mathsf{PEB}}{\partial\theta_i}(\tilde{\boldsymbol{\theta}}) = 0$. From (31) this means that $\Im\left\{\mathbf{z_i}(\tilde{\boldsymbol{\theta}})\right\} = 0$ of all i, i.e., all $\mathbf{z_i}$ lie on the real axis.

Candidates for minima will also be such that the second derivatives of the PEB will be positive. From (35) this implies that in addition $\Re\left\{\mathbf{z_i}(\tilde{\boldsymbol{\theta}})\right\} \leq 0$ of all i, i.e., all $\mathbf{z_i}$ lie on the *negative* real axis. □

The following lemma proves that RELOCATE actually converges to the stationary points that are candidates for minima.

LEMMA 3.11 CONVERGENCE OF RELOCATE. *RELOCATE converges to a stationary point $\tilde{\boldsymbol{\theta}} = \left(\tilde{\theta}_1, \ldots, \tilde{\theta}_n\right)$, such that all $\mathbf{z_k}(\tilde{\boldsymbol{\theta}})$ lie on the negative real axis, or*

$$\Re\left\{\mathbf{z_k}(\tilde{\boldsymbol{\theta}})\right\} \leq 0 \quad \textit{and} \quad \Im\left\{\mathbf{z_k}(\tilde{\boldsymbol{\theta}})\right\} = 0 \quad \forall k = 1, \ldots, n. \tag{36}$$

PROOF. Coordinate descent algorithms are guaranteed to converge to some stationary point if the function to be minimized is continuously differentiable and if the minimum in step (2) is uniquely attained [Bertsekas 2003]. This is the case here as shown in Lemma 3.8, so RELOCATE converges to a stationary point. This stationary point will be such that all $\tilde{\theta}_k$ satisfy (27) and therefore all $\mathbf{z_k}(\tilde{\boldsymbol{\theta}})$ lie on the negative real axis, or $\Re\left\{\mathbf{z_k}(\tilde{\boldsymbol{\theta}})\right\} \leq 0$ and $\Im\left\{\mathbf{z_k}(\tilde{\boldsymbol{\theta}})\right\} = 0$ for all k (Corollary 3.9). □

RELOCATE therefore converges to stationary points that are candidates for minima (Corollary 3.10). Note however that such points may not be global minima. Consider for example the case with 3 sensors where $A_1 = A_2 = A_3 = 1$, so that $r^* = 0$. An optimal configuration is found at $\boldsymbol{\theta}^* = (\pi/3, \pi, -\pi/3)$ (which yields $r(\boldsymbol{\theta}^*) = 0 = r^*$). Suppose RELOCATE is started at $\boldsymbol{\theta}^1 = (0, 0, \pi/2)$. It is easy to see that $\mathbf{z_1}(\boldsymbol{\theta}^1) = \mathbf{z_2}(\boldsymbol{\theta}^1) = 0$ and $\mathbf{z_3}(\boldsymbol{\theta}^1) = -2$. All the $\mathbf{z_k}$ lie on the negative real axis, while $r(\boldsymbol{\theta}^1) = 1 > r^*$; the algorithm has converged to a suboptimal stationary point. In the next subsection an additional step will be added to RELOCATE in order to guarantee convergence to the *global* minimum.

3.4 RELOCATE for Constant Importance Weights

Let us now implement RELOCATE for the case of constant importance weights.

RELOCATE

—Define $r^* = \max(0, A_n - \sum_{k=1}^{n-1} A_k)$ and the convergence threshold ϵ. Set $p = 1$;
—Randomly initialize $\boldsymbol{\theta}^1 = (\theta_1^1, ..., \theta_n^1)$;
—While $\left(r\left(\boldsymbol{\theta}^p\right) - r^*\right)/r^* > \epsilon$, do:
(1) Choose i_p such that $i_p = \arg\min_{k=1...n}\{|A_k - |\mathbf{z_k}(\boldsymbol{\theta}^p)||\}$;
(2) Calculate $\theta_{i_p}^*$ according to (27);
(3) Set $\theta_{i_p}^{p+1} = \theta_{i_p}^*$ and $\theta_k^{p+1} = \theta_k^p$ for $k \neq i_p$, so that $\boldsymbol{\theta}^{p+1} = \left(\theta_1^p, \ldots, \theta_{i_p}^*, \ldots, \theta_n^p\right)$;
(4) $p \leftarrow p + 1$.
(5) If all $\mathbf{z_k}(\boldsymbol{\theta}^p)$ lie on the negative real axis, enter the INCREASE_RADIUS routine;
—Else, stop.

INCREASE_RADIUS routine:

(1) Write $r\left(\boldsymbol{\theta}^p\right)$ as $\sum_{k\in S} A_k - \sum_{k\in\overline{S}} A_k$;
(2) Let l and m be 2 distinct indices in S;
(3) Choose θ_l^{p+1} such that $|A_m - |\mathbf{z_m}(\theta_1^p, \ldots, \theta_l^{p+1}, \ldots, \theta_n^p)|| < \sum_{k\in S} A_k - \sum_{k\in\overline{S}} A_k$;
(4) $p \leftarrow p + 1$, select sensor m for relocation, and go to step (2) of RELOCATE.

Note that in step (1) of RELOCATE the sensor that yields the maximum decrease in error radius is chosen (see Corollary A.1 in Appendix 0**??**). Alternatively, the sensor chosen for relocation at iteration p could also be selected at random.

According to Lemma 3.11, steps (1)-(4) of RELOCATE converge to a stationary point such that all the $\mathbf{z_k}$ lie on the negative real axis. As we illustrated, however, some of these configurations are suboptimal. We show in Lemma 3.12 that step (5) enables RELOCATE to escape such suboptimal stationary points so that it converges to the *optimal* stationary point (which is guaranteed to exist), characterized by an error radius equal to r^*.

LEMMA 3.12 OPTIMAL CONVERGENCE OF RELOCATE. *RELOCATE converges to the global minimum:*

—*If* $A_n > \sum_{k=1}^{n-1} A_k$*, RELOCATE finds* $\boldsymbol{\theta}^*$ *such that* $r(\boldsymbol{\theta}^*) = A_n - \sum_{k=1}^{n-1} A_k$*;*
—*Otherwise, RELOCATE finds* $\boldsymbol{\theta}^*$ *such that* $r(\boldsymbol{\theta}^*) = 0$*.*

PROOF. The proof is given in Appendix B. □

Let us illustrate how the algorithm operates on an example where all $A_k = 1$. We first reproduce some of the key results derived in Appendix 0**??** and 0**??**.

—The $\mathbf{z_k}\left(\boldsymbol{\theta}^p\right)$ are vectors starting at $(0,0)$ and ending on the same circle of radius $r\left(\boldsymbol{\theta}^p\right)$, centered at $(-1,0)$ (Corollary 3.3);

—When sensor i_p is relocated in step (2) of RELOCATE, the corresponding $\mathbf{z_{i_p}}$ is rotated about $(0,0)$ so as to lie on the negative real axis (Corollary 3.9), while its magnitude $|\mathbf{z_{i_p}}|$ does not change (Corollary 3.4). Note also that although the other θ_k (for $k \neq i_p$) are unchanged in this process, the corresponding $\mathbf{z_k}$ rotate *and* change magnitude;

—If sensor i_p is relocated at iteration p, the error radius is equal to $|A_k - |\mathbf{z_{i_p}}(\boldsymbol{\theta}^p)||$. Once it is relocated on the real axis, the error radius can also be found by measuring the distance between the tip of $\mathbf{z_{i_p}}(\boldsymbol{\theta}^{p+1})$ and $(-1,0)$ (Corollary A.1).

On Figure 5 are plotted the vectors $\mathbf{z_k}$ for 3 iterations of RELOCATE when 5 sensors are to be optimally placed. At the first iteration (Fig. 5(a)) sensor 3 is selected, and the corresponding $\mathbf{z_3}$ is rotated by almost π to lie on the negative real axis (Fig. 5(b)). Throughout the process its magnitude remains 1.62 (note the change in the axes scale). However the error radius has decreased significantly, from 3.6 (in Fig. 5(a)) to 0.62 (Fig. 5(b)).

At the next iteration sensor 5 is selected for relocation and $\mathbf{z_5}$ is made to lie on the negative real axis as shown on Fig. 5(c). The error radius is decreased to 0.1 in the process. By repeating this procedure the error radius diminishes to zero and all the $\mathbf{z_k}$ converge to $(-1,0)$.

Note that at each iteration the sensor whose vector yields the largest decrease in error radius is selected, as specified by step (1) of RELOCATE (i.e. the one whose $|\mathbf{z_k}|$ is closest to 1). As can be seen on Fig. 5 sensor 3 is the first to be selected, then sensor 5 for the second iteration, and finally sensor 1 for the third iteration.

The final configuration of sensors is shown on Figure 6. The final PEB is equal to $0.8944m$, which is optimal since it is equal to the value of the PEB when $r = 0$ in (16). The sensors are evenly distributed around the agent. Note that any sensor could be moved by π without changing the PEB value, so other configurations are optimal as well.

3.5 Rate of Convergence

In the next 2 subsections we analyze the performance of RELOCATE. We will show that not only is RELOCATE guaranteed to find the global minimum, but it is also an *efficient* algorithm. In this subsection we derive an approximation to the expected rate of convergence of RELOCATE for the special case when $A_k = 1$ for all k. Again, we are able to derive these results by relying on the coordinate transform introduced earlier.

If sensor i is selected for relocation at iteration p, the new error radius is $r^{p+1} = |1 - |\mathbf{z_i}(\boldsymbol{\theta}^p)||$, which is obtained by rotating $\mathbf{z_i}$ until it lies on the negative real axis and then measuring the distance between the tip of the vector and -1 (Corollary A.1). Assume $r^p \ll 1$, so that $\mathbf{z_i}(\boldsymbol{\theta}^p)$ is close to the negative real axis as depicted in Figure 7. We can then approximate r^{p+1} by projecting $|\mathbf{z_i}(\boldsymbol{\theta}^p)|$ onto the real axis and measuring the distance

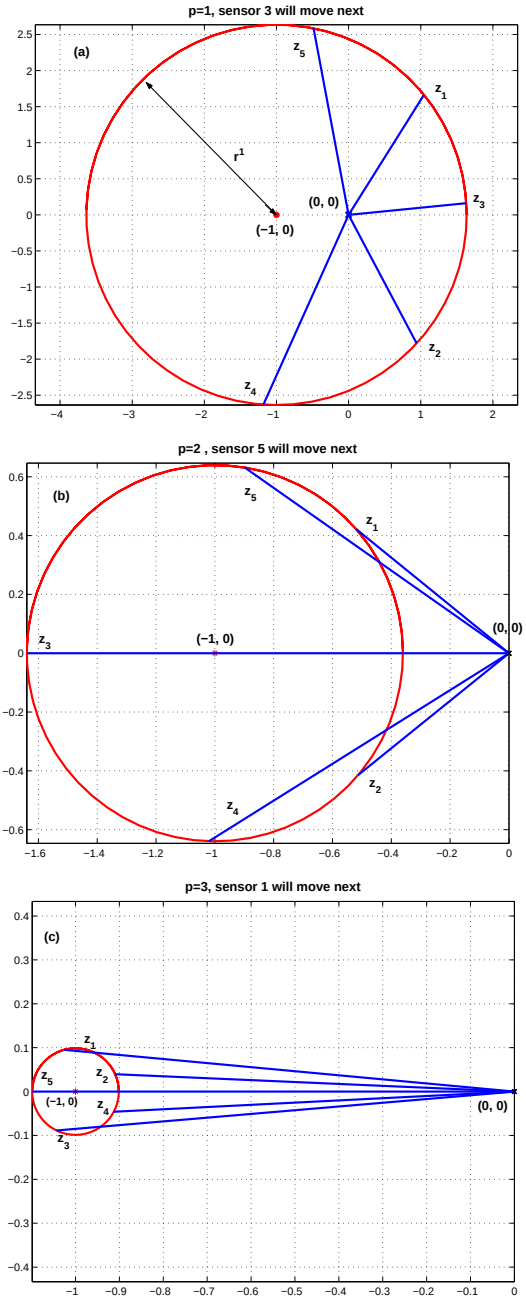

Fig. 5. Illustration of RELOCATE in the complex plane, after applying the coordinate transform. Plots of the $\mathbf{z_k}(\boldsymbol{\theta}^p)$ and of the circle of radius $r(\boldsymbol{\theta}^p)$ centered at -1 are shown for $p = 1, 2, 3$ for the case where all $A_k = 1$. The vector $\mathbf{z_k}$ selected at each step is rotated about the origin so as to lie on the negative real axis, which reduces the dimater of the circle $r(\boldsymbol{\theta}^p)$. Note that the sensor selected for relocation is the one with $|\mathbf{z_k}|$ closest to 1, so that the decrease in error radius r is maximum.

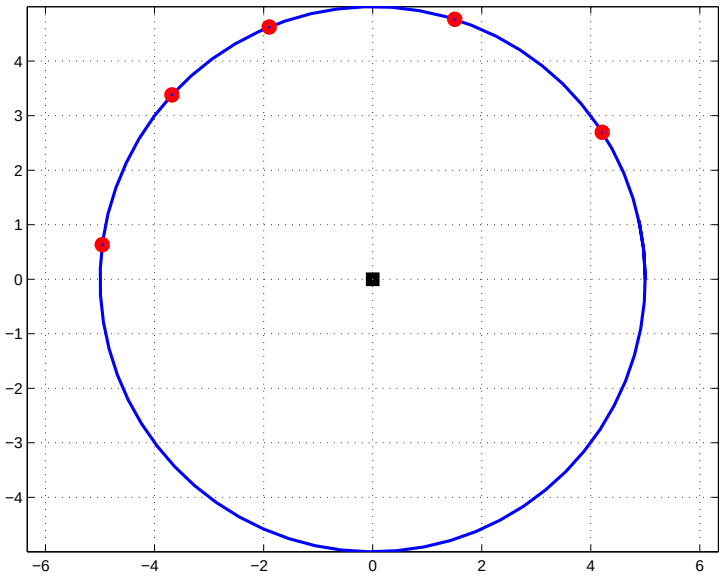

Fig. 6. Optimal configuration found by RELOCATE when 5 sensors are to be placed ona circle centered around the agent, with $A_k = 1$.

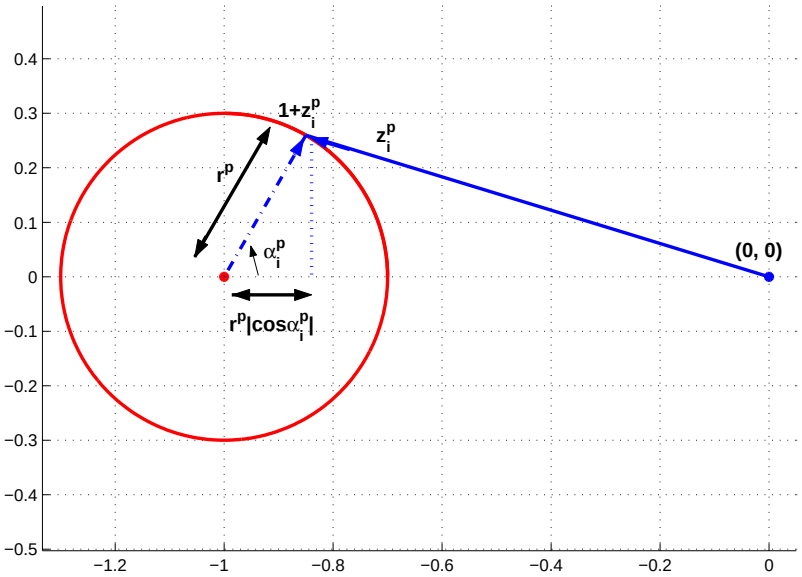

Fig. 7. Illustration of the approximation of $r^{p+1} = |1 - |\mathbf{z_i}(\boldsymbol{\theta}^p)||$ by $r^p|\cos\alpha_i^p|$.

between the tip of the projection and -1. This distance is equal to $r^p|\cos\alpha_i^p|$, where α_i^p is the argument of the vector $1 + \mathbf{z_i}(\boldsymbol{\theta}^p)$ (i.e. the angle it makes with the horizontal).

Because at iteration p the sensor with magnitude closest to 1 is selected for relocation,

the new error radius is equal to $r^{p+1} \simeq \min_{k=1\ldots n}(|\cos\alpha_k^p|)r^p$. If we define the rate of convergence τ^p as the ratio r^{p+1}/r^p, we then have

$$\tau^p \simeq \min_{k=1\ldots n}(|\cos\alpha_k^p|). \tag{37}$$

At iteration p one sensor (sensor i) lies on the negative real axis (the one relocated at iteration $p-1$), and let us assume that the $n-1$ other sensors have an equal probability of lying anywhere on the circle of radius r^p centered at -1, so that the α_k^p (for $k \neq i$) are uniform random variables distributed between 0 and 2π. We also assume that these α_k^p are independent. This is a questionable assumption since the $\mathbf{z_k}(\boldsymbol{\theta}^p)$ are not independent, but one that will enable us to obtain a closed-form solution to the expected rate of convergence which, as we will show, agrees with numerical examples.

The rate of convergence becomes a random variable τ, and its expected value will give the expected rate of convergence of RELOCATE. As shown in Appendix C, at each iteration p such that $r^p \ll 1$, the expected rate of decrease of the error radius can be approximated by

$$\mathbb{E}[\tau] \simeq \int_0^1 \left(\frac{2\cos^{-1}x}{\pi}\right)^{n-1} dx. \tag{38}$$

On average RELOCATE therefore converges *linearly*.

On Figure 8 this theoretical expected rate is plotted as a function of n, the number of sensors (dashed curve). It tends to 0 as n goes to infinity, which means that convergence is faster when more sensors are present. This is to be expected since the probability that $\mathbf{z_i}$ satisfies $|\mathbf{z_i}| = 1$ goes to 1 as the number of beacons is increased. We also performed 100 runs of RELOCATE for these values of n and computed the average ratio of decrease, once r^p was below 0.1. We see that as the number of beacons increases, the experimental average rate matches the theoretical value better.

3.6 Average Number of Iterations

Finally we use the previous result to estimate the average number of iterations required to reach a certain precision in PEB. When $A_k = 1\ \forall k$, $r^* = 0$ and the minimum value of the PEB for n sensors is equal to $\mathsf{PEB}^* = 2/\sqrt{n}$ (16). We can then express the relative error in PEB compared to the optimum value PEB^* as

$$\frac{\mathsf{PEB}^p - \mathsf{PEB}^*}{\mathsf{PEB}^*} = \frac{1}{\sqrt{1-(r^p/n)^2}} - 1, \tag{39}$$

so that it is approximately equal to $(r^p/n)^2/2$ for small values of r^p. Let s be the precision required, i.e., the maximum relative error permitted.

We assume we start the algorithm with a radius of 0.1, so that $r^1 \ll 1$. On average we then have $r^p = \tau^{p-1}r^1$. Achieving precision s will then require $1 + \frac{\log(10n\sqrt{2s})}{log\tau}$ iterations on average (not counting the iterations required to bring the radius below 0.1). This number is plotted as a function of the number of sensors for several values of the precision on Figure 9. We can see that once the error radius goes below 0.1, the algorithm converges in a few iterations even for high precision requirements. This is even more so as the number of sensors increases, which tends to speed up convergence.

In this section we proved that when a single agent location is considered and when the importance weights are constant, RELOCATE converges to the global minimum. We also

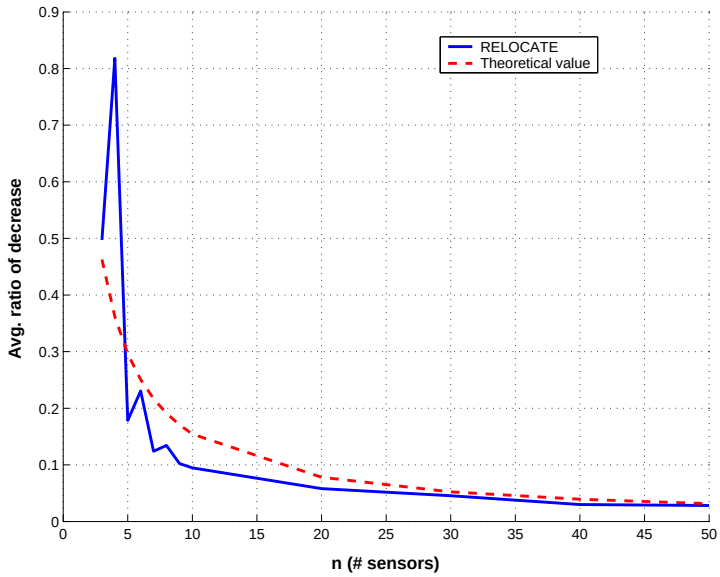

Fig. 8. Theoretical value of the expected rate of decrease of the error radius (dashed), and experimental value of this rate (solid). The experimental value converges to the theoretical one for large values of n.

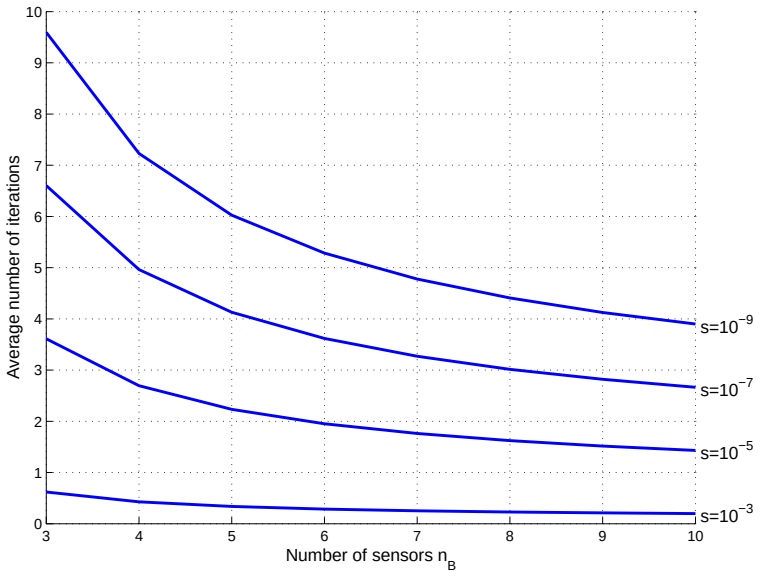

Fig. 9. Expected number of iterations once the error radius goes below 0.1 as a function of n. We have plotted this for several values of the precision s.

showed that it does so efficiently, in a few steps even for high accuracy requirement or large numbers of sensors. Fortunately RELOCATE can easily be applied to more complex cases where the importance weights depend on the sensor position, or when several agent

locations are of interest. Given the theoretical guarantees in this simple case, we now proceed with confidence in applying RELOCATE to those more complex cases. In the next section we apply it to the realistic case where the importance weights depend on where the sensors are located.

4. SINGLE AGENT LOCATION WITH VARYING IMPORTANCE WEIGHTS

So far the importance weights of the sensors were assumed constant, no matter where the sensors were. Although this assumption permitted us to solve the placement problem exactly, it is unlikely to be realistic in real-world scenarios. Since the signal-to-noise ratio (SNR) decreases exponentially with distance, the range measurements will be more accurate (i.e. have lower variance) if sensors and agent are close to one another. Likewise if the agent is inside a building, greater accuracy will be achieved if there is minimal obstruction between the two (as opposed to when several walls, machines, or other objects corrupt the signal). The result is that the importance weights of (8) will depend on the sensors' locations.

In this section we consider two cases. In the first one, the importance weights are piecewise constant functions of the angle. The second case is the most general, where the importance weights are allowed to vary arbitrarily. Note that in both cases we no longer have any guarantee of optimality, although in practice we do well.

4.1 Importance Weights as a Piecewise Constant Function of the Angle

Consider a scenario where the range measurement variance does not depend on the distance, but where obstacles, such as walls, block the line-of-sight (LOS) between the agent and the sensors at certain angles. At these angles, the sensor will be NLOS so its range measurements will be biased, which we modeled with $\beta > 0$ [Jourdan et al. 2006]. If we have a map of the area, we can predict what value β will take depending on the location of the sensor. The corresponding importance weights will then be a piecewise constant function of the angle. This is illustrated on Figure 10, where the agent is in the middle of a circular building, which contains several walls inside. The value of the importance weights on the building boundary changes depending on what obstructs the LOS between agent and sensor.

Let us then divide the interval $[0, 2\pi)$ into L arcs. On arc $C_l = [\underline{c_l}, \overline{c_l})$, the importance weight is constant, equal to A_l (obtained from (8)). The generic RELOCATE of Section 2.4 can be efficiently adapted to this case. The key is to note that solving step (2) is again easy. The following lemma shows that the minimum of the PEB along one coordinate is obtained at one of $2L + 2$ points: the two extremities of each arc, at the angle specified by (27), and at its symmetric with respect to the agent.

LEMMA 4.1. *Let* $\mathsf{PEB}(\theta_{i_p})$ *be the PEB when all the angles other than* θ_{i_p} *are kept constant. The angle* $\theta^*_{i_p}$ *minimizing* $\mathsf{PEB}(\theta_{i_p})$ *in step (2) of RELOCATE is given by*

$$\begin{aligned} \theta^*_{i_p} \;=\; & \arg\min\{\mathsf{PEB}(\tilde{\theta}_{i_p}), \mathsf{PEB}(\tilde{\theta}_{i_p} + \pi), \\ & \mathsf{PEB}(\underline{c_1}), \mathsf{PEB}(\overline{c_1}), ..., \mathsf{PEB}(\underline{c_L}), \mathsf{PEB}(\overline{c_L})\}, \end{aligned} \tag{40}$$

where $\tilde{\theta}_{i_p}$ *is the angle given by (27).*

PROOF. The proof is given in Appendix D. □

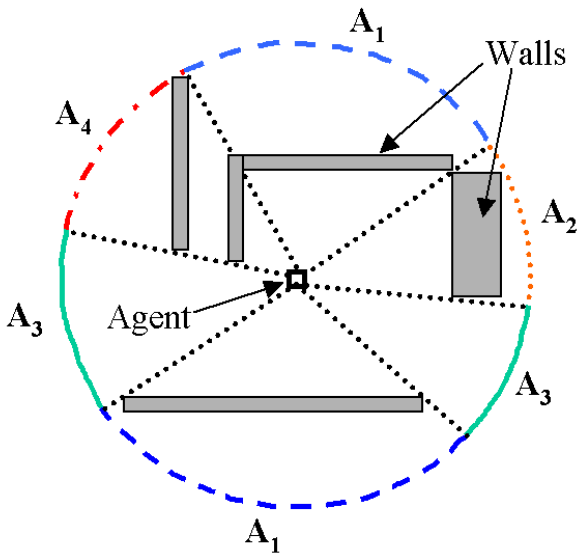

Fig. 10. An agent is located in the middle of a circular building, which contains several walls. The importance weights take a finite number of values (4 in this example, from A_1 to A_4), which reflect the different propagation environments caused by the obstacles.

This result makes step (2) of RELOCATE easy to solve, so that RELOCATE can again be applied to this problem efficiently. There is no longer any guarantee of global convergence however, but since the algorithm is fast it can be restarted several times from different initial conditions, to eliminate local minima.

Figure 11 illustrates a typical result. In this case the internal properties of the building result in 6 different importance weights at the boundary, represented by arcs of different colors. RELOCATE places 5 sensors on the boundary in order to optimally localize an agent placed at the center. Results show that RELOCATE places sensors on arcs with larger importance weight (sensors 1 through 4 are on the arc with $A_6 = 0.87$, sensor 5 is on the one with $A_2 = 0.60$), while spreading them in order to get range measurements from different viewpoints. RELOCATE tries to strike the optimal balance between spatial diversity (well-distributed measurement viewpoints) and measurement quality (arcs with large importance weights). Note that in this particular case all the sensors are located at the extremities of the arcs.

4.2 Importance Weights as an Arbitrary Function of the Angle

Consider the same scenario as before, except that now the range measurement variance increases with the distance to the agent as in (2). To be general we assume that α and β can also be arbitrary functions of the sensor location. The importance weights given by (8) can then be any function of the angle. This is the most general case for a single agent location, where the range measurement variance increases with the distance (possibly with different path-loss exponents), and where the sensors become NLOS at certain locations so that $\beta > 0$. Unfortunately this also implies that there is no longer any analytical solution to the minimization of step (2) of RELOCATE, so it must be solved numerically.

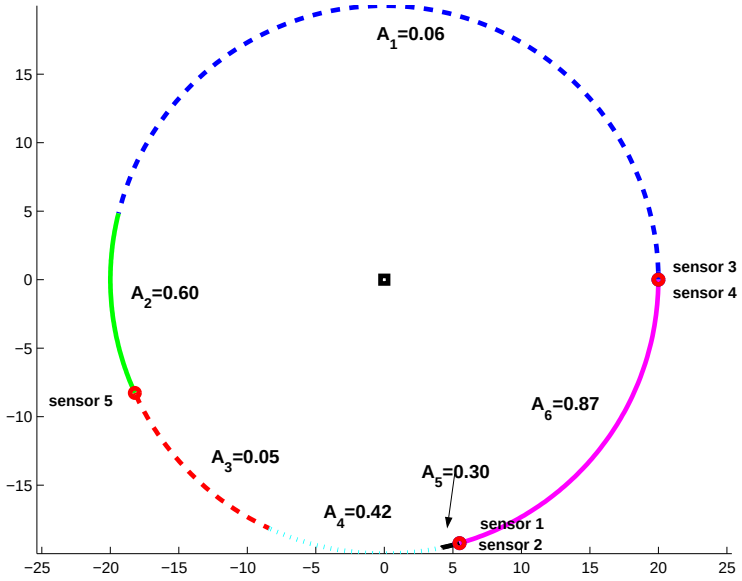

Fig. 11. Example of RELOCATE when the importance weights are a piecewise constant function of the angle, as illustrated on Figure 10. Sensors tend to be placed on arcs with larger weight, while maintaining some spatial diversity in their placement.

Let us consider a square area as shown on Figure 12, characterized by $\beta = 0$ and $\alpha = 0$, $\alpha = 0.2$ and $\alpha = 2$. The configurations for 6 sensors obtained through RELOCATE are shown for the cases where the agent is at the center (a)-(c) and at the lower left (d)-(f) of the area. When $\alpha = 0$ the sensors are scattered all around the agent. Note that by symmetry there are many sensor configurations that minimize the PEB in this case. However as α increases they tend to bunch together, so that when $\alpha = 2$ the sensors are evenly split into 2 clusters. We can see here again that RELOCATE strikes the optimal balance between spatial diversity and range measurement quality in order to minimize the PEB. The sensors are placed close to the agent so that they get range measurements of good quality, while also taking those measurements from different viewpoints (a minimum of two distinct measurement locations are necessary to localize the agent in 2D).

5. MULTIPLE AGENT LOCATIONS

5.1 Results with Average PEB

So far we have considered placing sensors in order to minimize the PEB at a *single* location. However in real scenarios we will often want to ensure good localization everywhere in the area, or along a pre-planned path. There are several possible choices of metrics to capture this accuracy, but a natural choice adopted here is to minimize the *average* PEB over the area or the path. RELOCATE can be applied as before, except that in step (2) the average PEB is minimized.

To illustrate this we consider the same square area as before, except that now several agent locations are specified (denoted by squares on Figure 13). The sensor configurations given by RELOCATE for different agent locations are also shown. In Fig. 13(a) the agent

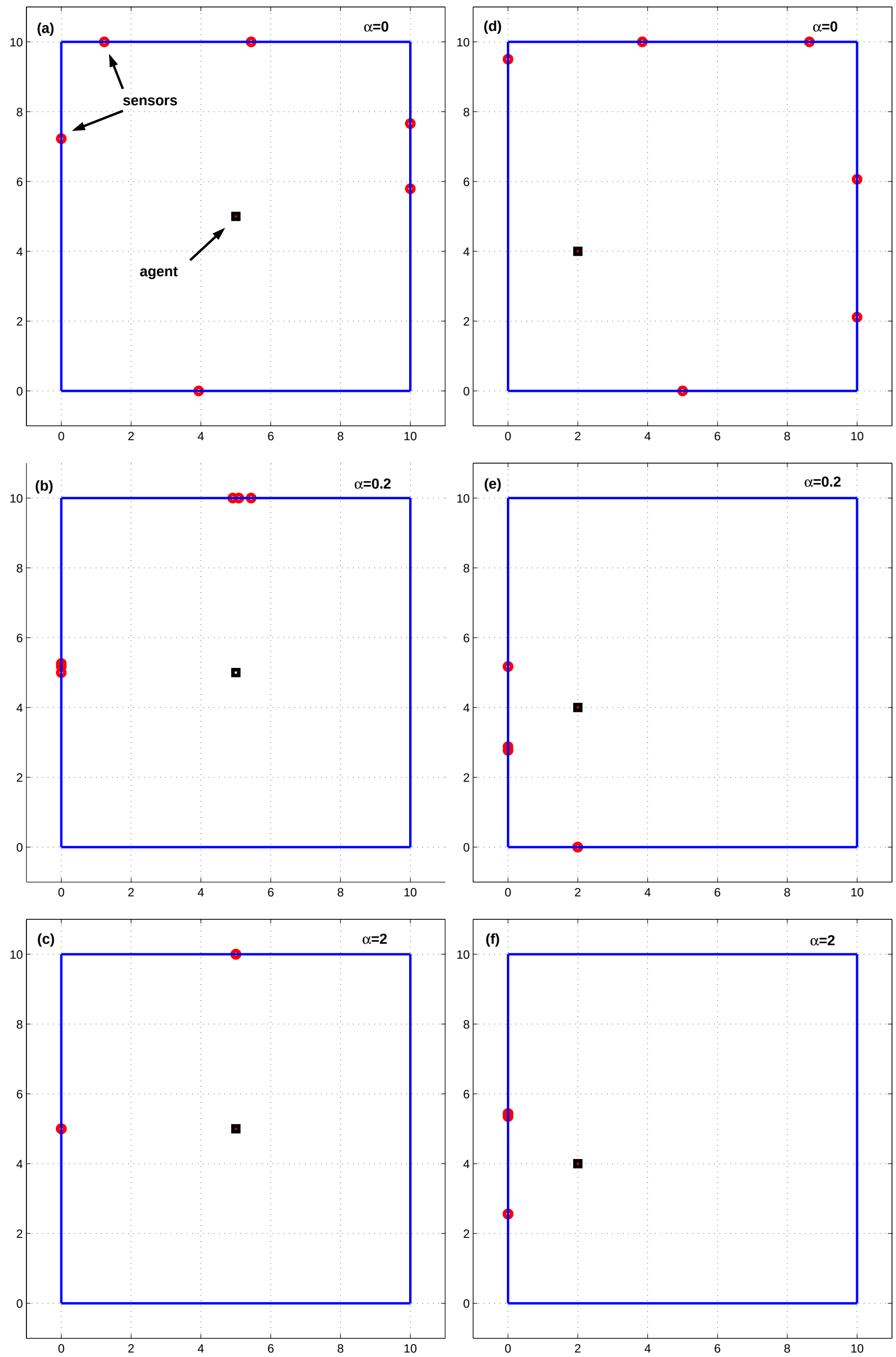

Fig. 12. Results of RELOCATE on a square boundary with the agent (denoted by a square) placed at the center (figures (a)-(c)) and at the lower left (figures (d)-(f)) of the boundary. $\beta = 0$ and α takes 3 values in each case: 0, 0.2, and 2. RELOCATE spreads the sensors around the agent when $\alpha = 0$ (since the distance to the agent does not matter), while as α increases RELOCATE strikes the optimal balance between spatial diversity and information quality (distance)

locations are evenly distributed throughout the area, which models the scenario where we want to ensure good localization everywhere (e.g. there is no pre-planned path). In this case RELOCATE places the sensors at regular intervals on the boundary, as intuition would suggest. Interestingly, results do not depend on the value of α.

Fig. 13(b)-(c) illustrate a scenario where we only want to ensure good localization in 2 parts of the building. For example the agent may know beforehand that it will only need to inspect 2 rooms inside a building, so good localization accuracy has to be provided there only. The configurations given by RELOCATE differ widely depending on α. If $\alpha = 2$, the sensors are evenly split between the two clusters of agent locations, and for each cluster they again strike the optimal balance between spatial diversity and measurement quality. For $\alpha = 0$ however, the measurement quality is uniform everywhere, so the sensors are more spread out.

Finally in Fig. 13(d)-(e) we consider a path inside the area. The agent already knows where it will travel, so it desires to place sensors so as to optimize the localization accuracy along that path. RELOCATE then concentrates the sensors on the wall close to the path when $\alpha = 2$, and spaces them evenly.

Results on the Fort McKenna MOUT Scenario

Let us consider an even more general scenario, where the agent can travel outside the building boundary. In particular we use a map of the Military Operations on Urbanized Terrain (MOUT) site at Fort McKenna to simulate a mission where an agent traveling through the area has to be accurately localized at all times, while the sensors can be placed on the exterior walls of different buildings. In this case the convexity assumption is violated, but as the results show RELOCATE still performs very well.

In the simulation shown on Figure 14 we assume that range measurements can only be made by sensors with LOS to the agent. This simulation can easily accommodate the case where range measurements can be made through buildings. For example NLOS measurements can be penalized by setting $\beta > 0$, so that the corresponding importance weight will be smaller than if the measurement was LOS.

The path of the agent is shown as black squares, and RELOCATE has to place 8 sensors accordingly. The resulting sensor placement shown on Fig. 14 indicates that RELOCATE performed its task well. In particular we note that every agent location is in view of at least 2 sensors, so that localization can be ensured at all times. These good results further indicate that RELOCATE is very flexible to more complex scenarios, where the *average* PEB is minimized and where the agent is not restricted to the interior of a boundary.

Note that RELOCATE can also easily deal with a *probabilistic* map of agent locations. In many scenarios the agent may not know beforehand where exactly it will go, but it may have an *a priori* density map of its future locations. The area can then be divided into a grid of agent locations, each assigned with a probability given by the density map. The *expected* PEB is then minimized in step (2) of RELOCATE.

5.2 Benchmarking RELOCATE with Simulated Annealing (SA)

Although there is no longer any guarantee of optimality or efficiency in the case of multiple agent locations with varying importance weights, we show in this section that RELOCATE is still efficient and gives results that are near-optimal. In particular we compare the performance of RELOCATE to that of Simulated Annealing (SA) [Kirkpatrick et al. 1983]. SA is a stochastic algorithm, so we expect it to avoid local minima and approach the global

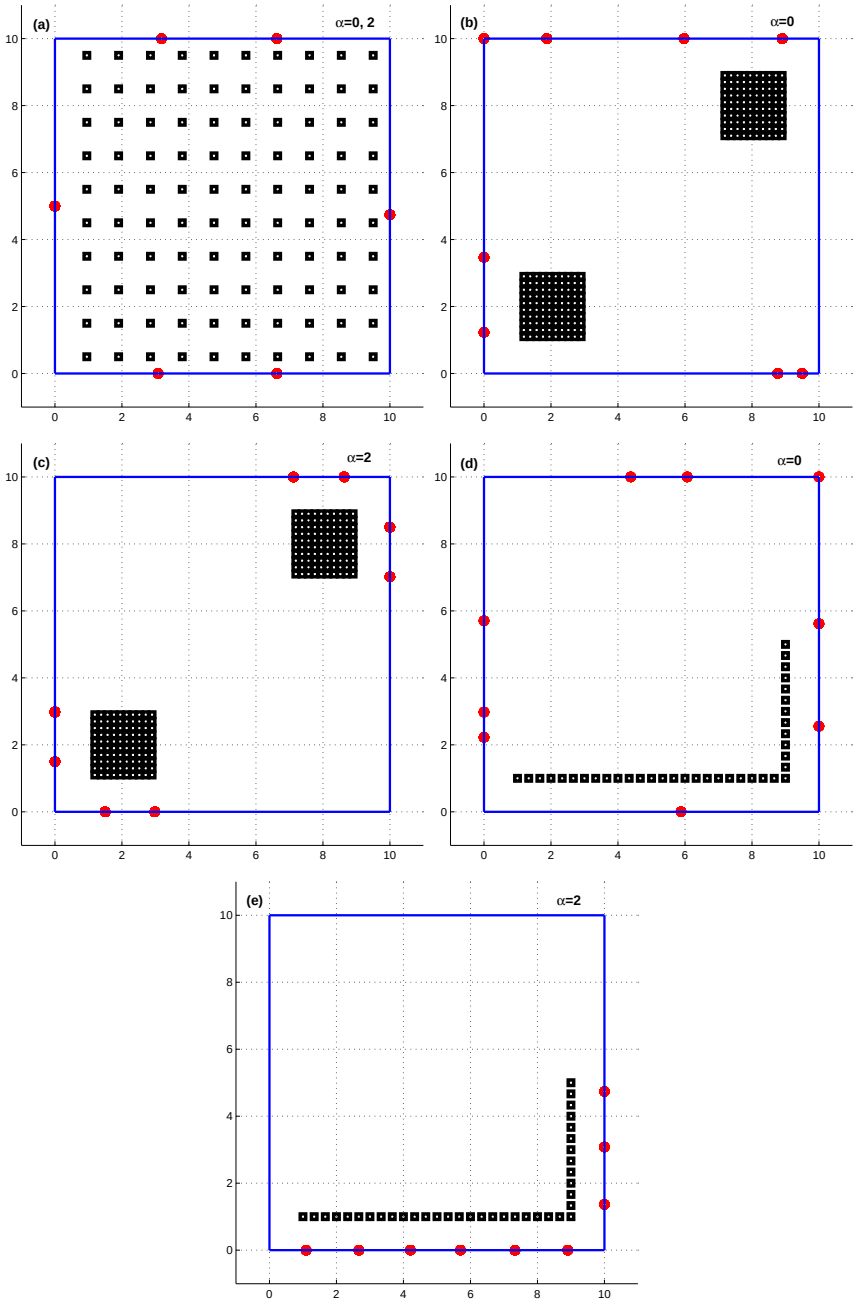

Fig. 13. Optimal configuration of sensors (denoted by red circles on the perimeter) given by RELOCATE for *several* agent locations (black squares). When the agent can be anywhere in the building (a), the sensors are evenly distributed on the building's boundary, whether $\alpha = 0$ or 2. The placement varies with α in the other two cases, when only portions of the building (b)-(c) or a path (d)-(e) must be covered.

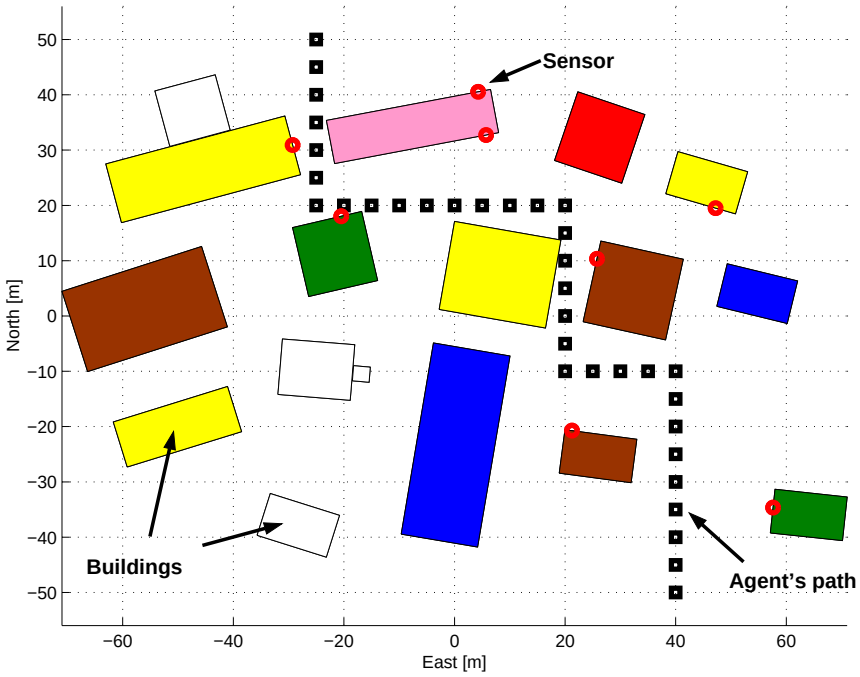

Fig. 14. Results of RELOCATE for the MOUT site of Fort McKenna. 8 sensors are placed on the boundary of buildings and can make range measurements to the agent when it is LOS. Note that every agent location is in view of at least 2 sensors, ensuring localization at all times. This is the most general case, with non-convex boundary and multiple agent locations

minimum. It is also an efficient heuristic algorithm, and it is particularly well-suited to such combinatorial optimization problems [Chiu and Lin 2004], so we use it to benchmark RELOCATE. We use the scenario of Fig. 13(d) to compare the two methods with 9 sensors to be placed. The average PEB obtained through RELOCATE ($\mathsf{PEB}_{\mathsf{RELOCATE}}$) and SA ($\mathsf{PEB}_{\mathsf{SA}}$) are compared over 100 simulation runs. In Figure 15, we plot the frequency histograms of the ratio $(\mathsf{PEB}_{\mathsf{SA}} - \mathsf{PEB}_{\mathsf{RELOCATE}})/\mathsf{PEB}_{\mathsf{RELOCATE}}$ for 3 sets of parameters of the SA that result in 3 different running times. The 3 SA parameterizations respectively took 0.22, 0.94, and 6.74 of the time it took for RELOCATE to complete. Positive values of the ratio indicate that the SA solution is worse than that of RELOCATE.

We see that although RELOCATE is a deterministic algorithm, it yields better results than SA most of the time. For the first two SA parameterizations, RELOCATE produces solutions that are always better than those of SA (the computational cost of SA and RELOCATE in Fig. 15(b) are almost similar). Only for longer runs does SA sometimes find better solutions than RELOCATE (Fig. 15(c)), but this happens rarely (8% of the time), while the improvement in average PEB is small (2% at most) and the time to completion is much larger than RELOCATE (6.74 more expensive computationally).

We proved before that RELOCATE finds the global minimum efficiently for a single agent and constant importance weights, and this study shows that even in more complex cases (multiple agent locations, varying weights) RELOCATE finds solutions very close to the global minimum. In addition, RELOCATE finds better solutions (indeed solutions

within 2% of the minimum given by SA) in less time than SA. We conclude that RELOCATE remains an efficient, near-optimal algorithm even for non-convex, realistic cases.

5.3 Benefit of Using a Placement Algorithm

Figures 13(d)-(e) illustrated how optimal sensor configurations vary with the value of α. In this case as α increases, sensors tend to gather closer to the path of the agent. A one-size-fits-all approach which would distribute the sensors evenly on the boundary (which we call UNIFORM) may therefore not be a good idea, at least in certain situations. Let us for example consider the agent path depicted in Fig. 13(e) with $\alpha = 2$. We compare three types of placement strategies along the boundary:

—Placement using RELOCATE

—Uniform placement (UNIFORM)

—Random placement (RANDOM)

For the last two strategies the results are averaged over 100 trials. We plot the average PEB resulting from these three methods in Figure 16 for different values of the number of sensors. We see that for a given number of sensors, RELOCATE yields an average PEB that is at least twice lower than that obtained by simply distributing the sensors evenly on the boundary. This is important in terms of the number of sensors needed to achieve a certain PEB. For example, to obtain an average PEB below $2mm$, 7 sensors are necessary using RELOCATE, whereas we need 15 with a uniform distribution, and 20 with random placement. Results when sensors are randomly placed are the worst, although not much worse than UNIFORM. The RELOCATE algorithm will therefore use significantly fewer sensors to achieve the same accuracy than a simple, one-size-fits-all approach. This demonstrates the importance of planning the sensors configuration optimally.

This is even more dramatically illustrated by considering the Fort McKenna scenario. For different number of sensors, we calculate the average PEB obtained by randomly placing the sensors on the perimeter of the buildings, versus placing them according to RELOCATE. The results are shown on Figure 17, where we plot the ratio between the average PEB obtained by random placement and that by RELOCATE. We can see that RELOCATE typically beats random placement by several orders of magnitude.

5.4 Achievability of the Bound

It is known that the Maximum Likelihood (ML) estimate converges to the CRB as the SNR tends to 0 [Van Trees 1968]. In our case this means that, when there is no bias, the PEB will be achievable as the variance σ^2 goes to 0. In this section we illustrate this result on a numerical example.

We consider the scenario depicted in Fig. 13(e), where the agent locations form a path that elbows alongside the building, while the sensors are placed either uniformly along the boundary or close to the agent locations. For each agent location, given a set of range measurements we calculate the ML estimate of the agent location by using a non-linear least-squares (NLLS) method [How and Deyst 2004]. By repeating this several times over one agent location, we can compute the Mean Square Error (MSE) of the position estimate, and compare it to the PEB at that location. Note that NLLS requires an initial position estimate, whereas the PEB assumes no *a priori* location information. The comparison between MSE and PEB is therefore not entirely fair, but it is still good because the initial position estimate given to NLLS is poor.

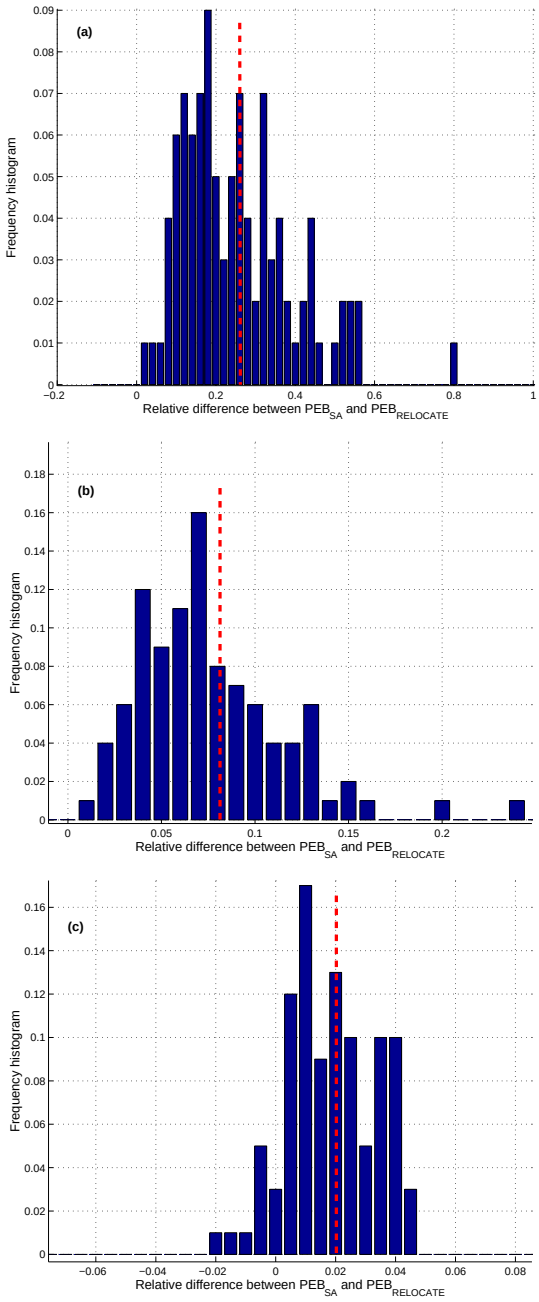

Fig. 15. Frequency histograms of the relative difference in PEB between the solution given by SA and RELOCATE, with the mean indicated by a dashed line. The SA respectively took a fraction of 0.22 (a), 0.94 (b), and 6.74 (c) of the time it took for RELOCATE to complete.

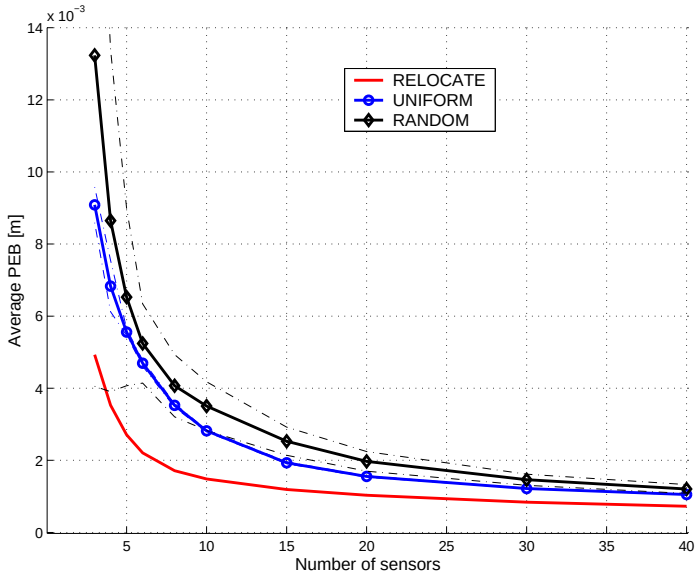

Fig. 16. Average PEB as a function of the number of sensors for the agent path depicted in the bottom plot of Figure 13 with $\alpha = 2$. The average PEB is obtained for 3 placement strategies: RELOCATE, UNIFORM, and RANDOM. The 1-σ envelope is indicated in dashed for the last two.

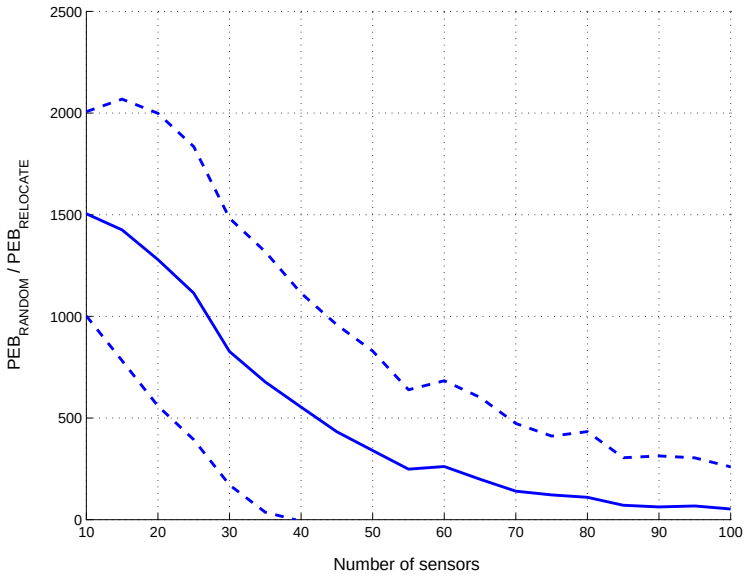

Fig. 17. Ratio of the average PEB obtained through random placement and that obtained through RELOCATE, as a function of the number of sensors placed in the Fort McKenna scenario. RELOCATE beats random placement by several orders of magnitude.

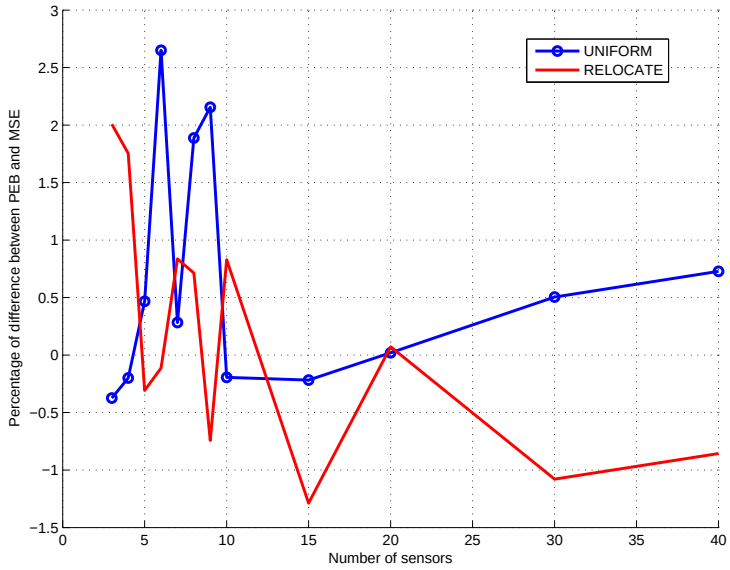

Fig. 18. Percentage of difference between the PEB and MSE as a function of the number of sensors deployed, when the sensors are placed using UNIFORM (circles) or RELOCATE. This shows that the PEB is an achievable lower bound (e.g. with a nonlinear least-squares estimator).

On Figure 18 we plot the percentage of difference between the average PEB and the average MSE over the path, as a function of the number of sensors deployed. We do this when the beacons are placed uniformly along the boundary (UNIFORM) and when they are clustered around the agent locations (RELOCATE). It can be seen that the average MSE and PEB are very close to one another (within 3% for all test points). The same was observed for the other configurations. The average MSE can actually be smaller than the PEB (positive values on Fig. 18), which can be explained by the fact that NLLS requires an initial position estimate, so it has more "knowledge" than what the PEB accounts for. In any case we conclude that, at least in some special cases when the bias is absent, the PEB will be close to achievable, so its actual value can be used as well. For example, if a certain localization accuracy is required, the PEB value can be used as an engineering tool to indicate whether more beacons should be deployed.

6. CONCLUSION

Although metrics based on the Information Inequality are widely used in the literature to measure the quality of sensor configurations for localization, there have only been a few papers on how to optimally place the sensors to guarantee good localization. In this paper we have proposed RELOCATE, an iterative algorithm that minimizes the Position Error Bound (PEB). We proved that it converges to the global minimum when the range measurements are unbiased and have constant variances, and we have derived its expected rate of convergence.

We have also shown that it can easily be extended to more realistic cases, where the quality of the range measurements depends on the sensors location. We have also applied RELOCATE to the optimal placement of sensors in order to minimize the *average* PEB

over multiple agent locations. In all cases RELOCATE attempts to strike a good balance between range measurement quality and spatial diversity. Those results have also shown that the optimal configuration of the sensors strongly depends on how the environment affects the quality of the range measurements. A one-size-fits-all placement strategy is therefore inappropriate, a point we illustrated by showing that using RELOCATE can significantly reduce the number of sensors needed to achieve a given accuracy requirement.

We have also shown that RELOCATE converges to solutions that are very close to the global minimum, and that it achieves these results efficiently when compared to Simulated Annealing. This algorithm therefore provides an efficient and flexible solution to the problem of designing sensor networks used for localization.

APPENDIX

A. COROLLARY OF LEMMA 3.8

COROLLARY A.1. *If sensor i_p is selected for relocation at iteration p, the error radius $r(\boldsymbol{\theta}^{p+1})$ after relocation will be equal to $|A_{i_p} - |\mathbf{z_{i_p}}(\boldsymbol{\theta}^p)||$*

PROOF. Since relocating sensor i_p makes $\mathbf{z_{i_p}}$ lie on the negative real axis (Corollary 3.9), the result is a direct consequence of Corollary 3.5. □

Given the n $\mathbf{z_k}(\boldsymbol{\theta}^p)$ at iteration p, we can therefore easily calculate the error radius resulting in relocating any of the sensors, so that the decrease in error radius can be predicted beforehand.

B. PROOF OF LEMMA 3.12: OPTIMAL CONVERGENCE OF RELOCATE

PROOF. For a given value of $\boldsymbol{\theta}^p$, we write $r^p \triangleq r(\boldsymbol{\theta}^p)$, $\mathbf{r}^p \triangleq \mathbf{r}(\boldsymbol{\theta}^p)$, and $\mathbf{z_k}^p \triangleq \mathbf{z_k}(\boldsymbol{\theta}^p)$ for all k and p.

Suppose that at iteration p RELOCATE produces a configuration $\boldsymbol{\theta}^p$ such that all $\mathbf{z_k}^p$ are on the negative real axis, while $r^p > r^*$. We first note that if nothing is done, the algorithm "stalls" at this point: because RELOCATE is a coordinate descent algorithm, it stops yielding improved results once a stationary point is reached (Lemma 3.11).

But we will show that by entering the INCREASE_RADIUS routine in step (5), the algorithm escapes this stationary point (notably by finding a configuration that is not stationary and has a radius strictly smaller). We also will show that step (5) can only be satisfied a finite number of times, so that is there are only a finite number of suboptimal stationary points. This implies that RELOCATE will not stop until it reaches an *optimal* stationary point. We show that this optimal stationary point is that with error radius equal to r^*.

Let us then assume that all the $\mathbf{z_k}^p$ lie on the negative real axis. By Corollary 3.5 we then have $r^p = |A_k - |\mathbf{z_k}^p||$. Since in addition the $\mathbf{z_k}^p$ are negative real numbers, we either have $r^p = A_k + \mathbf{z_k}^p$ or $r^p = -A_k - \mathbf{z_k}^p$. But by (14) we also know that $e^{-2j\theta_k^p}\mathbf{r}^p = \mathbf{z_k}^p + A_k$. Combining these we conclude that we must have

$$\frac{\mathbf{r}^p}{r^p} = \begin{cases} e^{2j\theta_k^p} & \text{or} \\ -e^{2j\theta_k^p}, \end{cases} \tag{41}$$

so that the angles θ_k^p are equal modulo $\pi/2$. There therefore exists a partition $(S, \overline{S})$ of $\{1, \ldots, n\}$ such that (12) can be written

$$r^p = \sum_{k \in S} A_k - \sum_{k \in \overline{S}} A_k. \tag{42}$$

Without loss of generality we assume that $\theta_k^p = 0$ for $k \in S$, and $\theta_k^p = \pi/2$ for $k \in \overline{S}$. We therefore have $\mathbf{r}^p = r^p$. Step (1) of INCREASE_RADIUS is therefore feasible.

The set S cannot be empty, otherwise r^p would be negative. Suppose that S is a singleton, so that $r^p = A_S - \sum_{k\in\overline{S}} A_k$. This is only possible (i.e. it is only positive) if $S = \{n\}$ and $A_n > \sum_{k=1}^{n-1} A_k$. But in that case $r^* = A_n - \sum_{k=1}^{n-1} A_k$ and $r^p = r^*$, which contradicts our assumption. S must then have at least 2 elements, so step (2) of INCREASE_RADIUS is feasible. Let l and m be 2 distinct indices of S.

Our strategy is as follows. The error radius cannot be reduced by relocating one sensor, which is what the normal operation of RELOCATE does. Instead we will relocate sensor l to a location different than that given by (27). This will result in an error radius r^{p+1} greater than r^p. But then we will show that relocating sensor m according to (27) will yield an error radius r^{p+2} such that $r^{p+2} < r^p$.

Assume then that at iteration p we relocate sensor l to θ_l. As a shorthand notation we write ${\mathbf{z}_\mathbf{m}}^{p+1}(\theta_l) \triangleq \mathbf{z}_\mathbf{m}(\theta_1^p, \ldots, \theta_l, \ldots, \theta_n^p)$. At iteration $p+1$ sensor m will in turn be relocated, this time to a θ_m^{p+2} given by (27). According to Corollary 3.5 the resulting error radius at iteration $p+2$ is then equal to $|A_m - |{\mathbf{z}_\mathbf{m}}^{p+1}(\theta_l)||$ (i.e. the actual value of θ_m^{p+2} does not matter, what matters is the fact that by (27) $\mathbf{z}_\mathbf{m}(\boldsymbol{\theta}^{p+2})$ will lie on the negative real axis).

Let us then study how $r^{p+2}(\theta_l) = |A_m - |{\mathbf{z}_\mathbf{m}}^{p+1}(\theta_l)||$ varies as a function of θ_l (where we have made the dependence of r^{p+2} on θ_l explicit). In particular we want to show that there exists a θ_l such that $r^{p+2}(\theta_l) < r^p$. This is true if and only if

$$A_m \in \left(\min_{\theta_l\in[0,\pi)} |{\mathbf{z}_\mathbf{m}}^{p+1}(\theta_l)| - r^p, \quad \max_{\theta_l\in[0,\pi)} |{\mathbf{z}_\mathbf{m}}^{p+1}(\theta_l)| + r^p \right). \tag{43}$$

We write $a_1 = \min_{\theta_l\in[0,\pi)} |{\mathbf{z}_\mathbf{m}}^{p+1}(\theta_l)| - r^p$ and $a_2 = \max_{\theta_l\in[0,\pi)} |{\mathbf{z}_\mathbf{m}}^{p+1}(\theta_l)| + r^p$. Note that $a_2 \geq a_1$ since r^p is non-negative. There therefore exists a θ_l such that $r^{p+2}(\theta_l) < r^p$ if and only if the interval $\mathcal{A} \triangleq (a_1, a_2)$ contains A_m.

Let us first obtain ${\mathbf{z}_\mathbf{m}}^{p+1}(\theta_l)$ as an explicit function of θ_l. We have

$$\begin{aligned}
{\mathbf{z}_\mathbf{m}}^{p+1}(\theta_l) &= e^{-2j\theta_m^p}\mathbf{r}(\boldsymbol{\theta}^{p+1}) - A_m && (44)\\
&= e^{-2j\theta_m^p}\left(\sum_{k\neq l} A_k e^{-2j\theta_k^p} + A_l e^{-2j\theta_l}\right) - A_m && (45)\\
&= e^{-2j\theta_m^p}\left(\mathbf{r}^p - A_l e^{-2j\theta_l^p} + A_l e^{-2j\theta_l}\right) - A_m && (46)\\
&= r^p - A_m + A_l\left(e^{-2j\theta_l} - 1\right), && (47)
\end{aligned}$$

where the first equation is from (14), in the second we use (12) to expand the error vector, in the third we write $\mathbf{r}^p = \sum_{k=1}^n A_k e^{-2j\theta_k^p}$, and in the fourth we use the fact that $\theta_l^p = \theta_m^p = 0$ since l and m belong to S. The extrema of $|{\mathbf{z}_\mathbf{m}}^{p+1}(\theta_l)|$ are thus found at $\theta_l = 0$ and $\theta_l = \pi/2$, and take the following values

—$|{\mathbf{z}_\mathbf{m}}^{p+1}(0)| = |r^p - A_m|$;
—$|{\mathbf{z}_\mathbf{m}}^{p+1}(\pi/2)| = |r^p - A_m - 2A_l|$.

We can now study the interval $\mathcal{A}$ for the different cases, remembering that $A_l > 0$, $A_m > 0$, and $r^p > 0$.

—$r^p - A_m - A_l \geq 0$
In this case we have $|\mathbf{z_m}^{p+1}(0)| = r^p - A_m$ and $|\mathbf{z_m}^{p+1}(\pi/2)| = |r^p - A_m - 2A_l|$. Since

$$|\mathbf{z_m}^{p+1}(0)| - |\mathbf{z_m}^{p+1}(\pi/2)| = r^p - A_m - |r^p - A_m - 2A_l| \quad (48)$$
$$= 2A_l, \text{ or } 2(r^p - A_m - A_l), \quad (49)$$

where both are non-negative, we conclude that the maximum of $|\mathbf{z_m}^{p+1}(\theta_l)|$ is achieved for $\theta_l = 0$, and the minimum for $\theta_l = \pi/2$.
—If $r^p - A_m - 2A_l \geq 0$, then $|\mathbf{z_m}^{p+1}(\pi/2)| = r^p - A_m - 2A_l$ and:

$$\begin{cases} a_1 = (r^p - A_m - 2A_l) - r^p < 0 < A_m \\ a_2 = r^p - A_m + r^p = 2(r^p - A_m) + A_m > A_m \end{cases} \quad (50)$$

where the second inequality holds because $r^p - A_m \geq A_l > 0$.
—If $r^p - A_m - 2A_l < 0$, then $|\mathbf{z_m}^{p+1}(\pi/2)| = -(r^p - A_m - 2A_l)$ and:

$$\begin{cases} a_1 = -(r^p - A_m - 2A_l) - r^p = -2(r^p - A_m - A_l) - A_m < 0 < A_m \\ a_2 = r^p - A_m + r^p = 2(r^p - A_m) + A_m > A_m \end{cases} \quad (51)$$

In both cases, we have $a_1 < A_m < a_2$.

—$r^p - A_m - A_l < 0$
In this case we have $|\mathbf{z_m}^{p+1}(0)| = |r^p - A_m|$ and $|\mathbf{z_m}^{p+1}(\pi/2)| = -(r^p - A_m - 2A_l)$. Since

$$|\mathbf{z_m}^{p+1}(\pi/2)| - |\mathbf{z_m}^{p+1}(0)| = -(r^p - A_m - 2A_l) - |r^p - A_m| \quad (52)$$
$$= -2(r^p - A_m - A_l), \text{ or } 2A_l, \quad (53)$$

where both are non-negative, we conclude that the maximum of $|\mathbf{z_m}^{p+1}(\theta_l)|$ is achieved for $\theta_l = \pi/2$, and the minimum for $\theta_l = 0$.
—If $r^p - A_m \geq 0$, then $|\mathbf{z_m}^{p+1}(0)| = r^p - A_m$ and:

$$\begin{cases} a_1 = (r^p - A_m) - r^p < 0 < A_m \\ a_2 = -(r^p - A_m - 2A_l) + r^p = A_m + 2A_l > A_m \end{cases} \quad (54)$$

—If $r^p - A_m < 0$, then $|\mathbf{z_m}^{p+1}(0)| = -(r^p - A_m)$ and:

$$\begin{cases} a_1 = -(r^p - A_m) - r^p = -2r^p + A_m < A_m \\ a_2 = -(r^p - A_m - 2A_l) + r^p = A_m + 2A_l > A_m \end{cases} \quad (55)$$

where the first inequality holds because $r^p > 0$.
In both cases, we have again $a_1 < A_m < a_2$.

We conclude that in any case $A_m \in \mathcal{A}$ so that (43) is satisfied. Step (3) of INCREASE_RADIUS is therefore feasible. Let θ_l^{p+1} receive a value such that $|A_m - |\mathbf{z_m}^{p+1}(\theta_l^{p+1})|| < r^p$ (just choose $\theta_l^{p+1} = 0$ or $\pi/2$ depending on the relative values of r^p, A_l and A_m). At iteration $p+1$ relocating sensor m according to (27) will then be guaranteed to yield an error radius r^{p+2} strictly smaller than r^p.

Each time the INCREASE_RADIUS routine is entered, a smaller radius can therefore be found. But in order to enter the INCREASE_RADIUS routine in the first place, we have also shown that $\boldsymbol{\theta}$ must be such that (42) is verified. Since there are only a finite number of partitions of $(1, \ldots, n)$, the INCREASE_RADIUS routine can only be entered a

finite number of times. We conclude that the error radius is guaranteed to decrease until it converges to its optimal value r^*. □

A consequence of the convergence of RELOCATE to the global minimum is the following corollary, which strengthens Lemma 3.7.

COROLLARY B.1. *There exists $\boldsymbol{\theta}$ such that $r(\boldsymbol{\theta}) = 0$ if and only if $A_n \leq \sum_{k=1}^{n-1} A_k$.*

C. DERIVATION OF THE EXPECTED RATE OF CONVERGENCE OF RELOCATE

PROOF. For any iteration p, let $|\cos(\alpha_M)| = \min_{k \neq i} |\cos \alpha_k|$, $X_M = |\cos(\alpha_M)|$, and $X_k = |\cos(\alpha_k)|$ for all k. Note that the X_k are independent, identically distributed because of our assumptions. We have

$$\begin{aligned}
\mathbb{P}\{X_M \leq x\} &= 1 - \mathbb{P}\{X_M > x\} && (56)\\
&= 1 - \mathbb{P}\{(X_1 > x) \cap \ldots \cap (X_n > x)\} && (57)\\
&= 1 - \mathbb{P}\{X_1 > x\}^{n'} && (58)\\
&= 1 - (1 - \mathbb{P}\{X_1 \leq x\})^{n'}, && (59)
\end{aligned}$$

where $\mathbb{P}(A)$ denotes the probability of event A, and $n' = n - 1$. The pdf of X_M can be written as

$$f_{X_M}(x) = n'(1 - \mathbb{P}\{X_1 \leq x\})^{n'-1} f_X(x), \tag{60}$$

where $f_X(x)$ is the pdf of X_1. The statistics of X_1 are

$$\begin{aligned}
\mathbb{P}\{X_1 \leq x\} &= \mathbb{P}\{|\cos\alpha| \leq x\} && (61)\\
&= \mathbb{P}\{\cos\alpha \leq x \mid 0 \leq \alpha < \pi/2\} && (62)\\
&= 1 - \frac{2\cos^{-1} x}{\pi}. && (63)
\end{aligned}$$

The pdf of X_1 is then $f_X(x) = \frac{2}{\pi}\frac{1}{\sqrt{1-x^2}}$, so that

$$f_{X_M}(x) = n' \left(\frac{2}{\pi}\right)^{n'} \frac{\left(\cos^{-1} x\right)^{n'-1}}{\sqrt{1-x^2}}. \tag{64}$$

We can now calculate the expected value of X_M

$$\begin{aligned}
\mathbb{E}[X_M] &= \int_0^1 x f_{X_M}(x) dx && (65)\\
&= \left(\frac{2}{\pi}\right)^{n'} \int_0^1 n' \frac{\left(\cos^{-1} x\right)^{n'-1}}{\sqrt{1-x^2}} dx. && (66)\\
& && (67)
\end{aligned}$$

By integrating by parts and replacing n' by $n - 1$ we obtain the desired result

$$\mathbb{E}[\tau] = \int_0^1 \left(\frac{2\cos^{-1} x}{\pi}\right)^{n-1} dx. \tag{68}$$

□

D. PROOF OF LEMMA 4.1: MINIMIZATION OF STEP (2) FOR PIECEWISE CONSTANT IMPORTANCE WEIGHTS

PROOF. Let $c_k = \cos\theta_k$ and $s_k = \sin\theta_k$ for any k. $\mathsf{PEB}(\theta_{i_p})$ can be written as

$$\begin{aligned}\mathsf{PEB}(\theta_{i_p}) &= \sqrt{\frac{\sum_{k\neq i_p} A_k + A_{i_p}(\theta_{i_p})}{(\sum_{k\neq i_p} A_k c_k^2 + A_{i_p} c_{i_p}^2)(\sum_{k\neq i_p} A_k s_k^2 + A_{i_p} s_{i_p}^2) - (\sum_{k\neq i_p} A_k c_k s_k + A_{i_p} c_{i_p} s_{i_p})^2}} \\ &= \sqrt{\frac{\overline{A_{i_p}} + A_{i_p}(\theta_{i_p})}{\overline{A_{i_p}}/\overline{\mathsf{PEB}}_{i_p}^2 + A_{i_p}(\sum_{k\neq i_p} A_k (c_k^2 s_{i_p}^2 + s_k^2 c_{i_p}^2 - 2c_k s_{i_p} s_k c_{i_p}))}} \\ &= \overline{\mathsf{PEB}}_{i_p} \sqrt{\frac{\overline{A_{i_p}} + A_{i_p}(\theta_{i_p})}{A_{i_p}(\theta_{i_p}) G(\theta_{i_p}) \overline{\mathsf{PEB}}_{i_p}^2 + \overline{A_{i_p}}}}, \end{aligned} \tag{69}$$

where $\overline{A_{i_p}} = \sum_{k\neq i_p} A_k(\theta_k)$, $\overline{\mathsf{PEB}}_{i_p}$ is the PEB when sensor i_p is removed, that is

$$\overline{\mathsf{PEB}}_{i_p} = \sqrt{\frac{\sum_{k\neq i_p} A_k(\theta_k)}{\sum_{k\neq i_p} A_k(\theta_k) c_k^2 \sum_k A_k(\theta_k) s_k^2 - (\sum_{k\neq i_p} A_k(\theta_k) c_k s_k)^2}}, \tag{70}$$

and where

$$G(\theta_{i_p}) = \sum_{k\neq i_p} A_k \sin^2(\theta_{i_p} - \theta_k). \tag{71}$$

If $A_{i_p}(\theta_{i_p})$ were constant with respect to θ_{i_p}, then $\mathsf{PEB}(\theta_{i_p})$ would be similar to the case considered in Section 3, with 2 minima and 2 maxima in $[0, 2\pi)$ (see Figure 4). However because A_{i_p} is piecewise constant, $\mathsf{PEB}(\theta_{i_p})$ is discontinuous at the L arc transitions, as shown on Figure 19.

For each arc there are several possibilities:

—$\mathsf{PEB}(\theta_{i_p})$ is monotonous, in which case the minimum PEB on this arc occurs at one of its boundary;

—$\mathsf{PEB}(\theta_{i_p})$ is not monotonous on this arc:

  —If there is no inflection point that is a minimum, the minimum PEB on this arc occurs at one of its boundary;

  —If there is at least one inflection point that is a minimum, the minimum PEB on this arc occurs at those. Its possible values are $\tilde{\theta_{i_p}}$ or $\tilde{\theta_{i_p}} + \pi$, given by (27).

In any case, to find the minimum of PEB we only need to test its value at the boundary points of each arc, and at $\tilde{\theta_{i_p}}$ and $\tilde{\theta_{i_p}} + \pi$. □

REFERENCES

ABEL, J. S. 1990. Optimal sensor placement for passive source localization. In *Proceedings of the IEEE International Conference on Acoustics, Speech, and Signal Processing*. Albuquerque, NM.

BAR-SHALOM, Y., LI, X. R., AND KIRUBARAJAN, T. 2001. *Estimation with Application to Tracking and Navigation*. Wiley, New York, NY.

BERTSEKAS, D. P. 2003. *Nonlinear Programming*. Athena Scientific, Belmont, MA.

BICKEL, P. J. AND DOKSUM, K. 2001. *Mathematical Statistics: Basic Ideas and Selected Topics*, second ed. Vol. 1. Prentice Hall, Upper Saddle River, NJ.

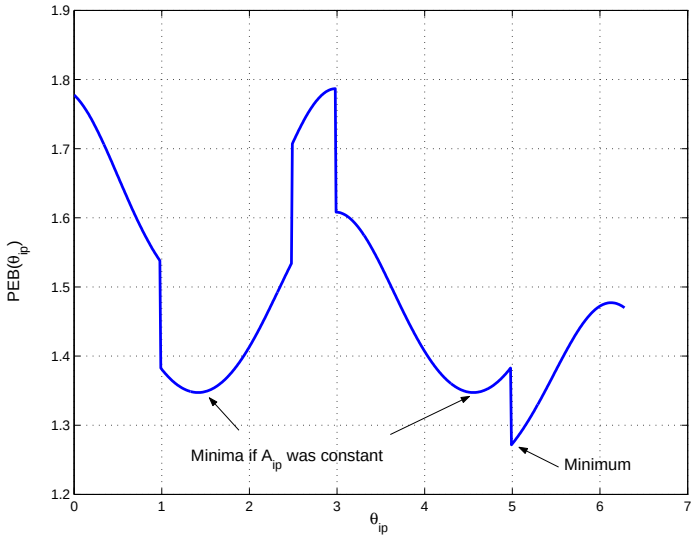

Fig. 19. When $A_{i_p}(\theta_{i_p})$ is piecewise constant, $\mathsf{PEB}(\theta_{i_p})$ shows discontinuity at the 4 transitions between arcs (compare to Fig. 4). The minimum may not be at one of the 2 points given by (27).

CASSIOLI, D., WIN, M. Z., AND MOLISCH, A. F. 2002. The ultra-wide bandwidth indoor channel: from statistical model to simulations. *20,* 6 (August), 1247–1257.

CHAFFEE, J. AND ABEL, J. 1994. GDOP and the Cramer-Rao bound. In *Proceedings of the Position, Location and Navigation Symposium (PLANS)*. Las Vegas, NV, 663–668.

CHIU, P. L. AND LIN, F. Y. S. 2004. A simulated annealing algorithm to support the sensor placement for target location. In *Proceedings of the CCECE*. Vol. 2. Niagara Falls, Ontario, 867–870.

FALSI, C., DARDARI, D., MUCCHI, L., AND WIN, M. Z. 2006. Time of arrival estimation for UWB localizers in realistic environments. In *Proceedings of the International Conference on Communications*. Istanbul, Turkey. to appear.

FOX, D., BURGARD, W., AND THRUN, S. 1999. Markov localization for mobile robots in dynamic environments. *Journal of Artificial Intelligence Research 11*, 391–427.

GEZICI, S., TIAN, Z., GIANNAKIS, G., KOBAYASHI, H., MOLISCH, A., POOR, H., AND SAHINOGLU, Z. 2005. Localization via ultra-wideband radios: a look at positioning aspects for future sensor networks. *IEEE Signal Processing Magazine 22*, 70–84.

HEGAZY, T. AND VACHTSEVANOS, G. 2003. Sensor placement for isotropic source localization. In *Proceedings of the Second International Workshop on Information Processing in Sensor Networks*. Palo Alto, CA.

HOW, J. P. AND DEYST, J. J. 2004. Advanced estimation for GPS and inertial navigation. MIT 16.324 class-notes.

JOURDAN, D. B., DARDARI, D., AND WIN, M. Z. 2006. Position error bound for UWB localization in dense cluttered environments. In *Proceedings of IEEE International Conference on Communications*. Istanbul, Turkey.

JOURDAN, D. B., DEYST, J. J., WIN, M. Z., AND ROY, N. 2005. Monte-Carlo localization in dense multipath environments using UWB ranging. In *Proceedings of IEEE International Conference on Ultra-Wideband*. Zurich, CH, 314–319.

KIRKPATRICK, S., GELATT, C. D., AND VECCHI, M. P. 1983. Optimization by simulated annealing. *Science 220, 4598,* 671–680.

LEE, J.-Y. AND SCHOLTZ, R. A. 2002. Ranging in a dense multipath environment using an UWB radio link. *IEEE Journal on Selected Areas in Communications 20,* 9 (December), 1677–1683.

LEONARD, J. J. AND DURRANT-WHYTE, H. F. 1992. *Directed Sonar Sensing for Mobile Robot Navigation*. Kluwer Academic Publishers, Boston, MA.

LEVANON, N. 2000. Lowest GDOP in 2-D scenarios. *IEE Proceedings-Radar, Sonar Navigation 147,* 3 (March), 149–155.

LOW, Z. N., CHEONG, J. H., LAW, C. L., NG, W. T., AND LEE, Y. J. 2005. Pulse detection algorithm for Line-of-Sight (LOS) UWB ranging applications. *IEEE Antennas and Wireless Propagation Letters 4*, 63–67.

MARTÍNEZ, S. AND BULLO, F. 2004. Optimal sensor placement and motion coordination for target tracking. *Automatica*. To appear.

MCKAY, J. AND PACHTER, M. 1997. Geometry optimization for GPS navigation. In *Proceedings of the 36th Conference on Decision and Control*. San Diego, CA.

MINVIELLE, P. 2005. Decades of improvements in re-entry ballistic vehicle tracking. *IEEE Aerospace and Electronic Systems Magazine, Part 1 20,* 8 (August), CF1–CF14.

SHENG, X. AND HU, Y. H. 2003. Sensor deployment for source localization in wireless sensor network system.

SINHA, A., KIRUBARAJAN, T., AND BAR-SHALOM, Y. 2004. Optimal cooperative placement of GMTI UAVs for ground target tracking. In *Proceedings of the IEEE Aerospace Conference*. Big Sky, MT.

SKOLNIK, M. L. 1980. *Introduction to Radar Systems*. McGraw-Hill, New York, NY.

SPILKER, JR., J. J. 1978. GPS signal structure and performance characteristics. *Journal of the Institute of Navigation 25,* 2 (Summer), 121–146.

TARDÓS, J. D., NEIRA, J., NEWMAN, P. M., AND LEONARD, J. J. 2002. Robust mapping and localization in indoor environments using sonar data. *International Journal of Robotics Research 21,* 4 (April), 311–330.

VAN TREES, H. L. 1968. *Detection, Estimation and Modulation Theory*. Wiley, New York, NY.

WIN, M. Z. AND SCHOLTZ, R. A. 1998a. On the energy capture of ultra -wide bandwidth signals in dense multipath environments. *2,* 9 (September), 245–247.

WIN, M. Z. AND SCHOLTZ, R. A. 1998b. On the robustness of ultra -wide bandwidth signals in dense multipath environments. *2,* 2 (February), 51–53.

WIN, M. Z. AND SCHOLTZ, R. A. 2002. Characterization of ultra -wide bandwidth wireless indoor communications channel: A communication theoretic view. *20,* 9 (December), 1613–1627.

YARLAGADDA, R., ALI, I., AL-DHAHIR, N., AND HERSHEY, J. 2000. GPS GDOP metric. *IEE Proceedings-Radar, Sonar Navigation 147,* 5 (May), 259–264.

ZHANG, H. 1995. Two-dimensional optimal sensor placement. *IEEE Transactions on Systems, Man, and Cybernetics 25,* 5 (May).